Reverse Osmosis Desalination and Hybrid Membrane Processes for Brine Treatment

by

Abdullah Albiladi

A thesis
presented to the University of Waterloo
in fulfillment of the
thesis requirement for the degree of
Master of Applied Science
in
Chemical Engineering (Water)

Waterloo, Ontario, Canada, 2019

Author's Declaration

I hereby declare that I am the sole author of this thesis. This is a true copy of the thesis, including any required final revisions, as accepted by my examiners.

I understand that my thesis may be made electronically available to the public.

Abstract

Waste from seawater reverse osmosis desalination processes is commonly referred to as brine which is one of the obstacles creating environmental and economic inefficiencies. The objective of this work is to simulate the hollow fiber reverse osmosis desalination membrane process to quantify its brine volume and concentration. Then, the pervaporation process and membrane distillation process are simulated to study and compare their brine treatment capabilities.

An accurate model is identified and used to represent the hollow fiber reverse osmosis process. Then, the models for pervaporation and membrane distillation are studied separately and the most accurate ones are selected to represent each process. After that, the models are arranged in an order to minimize brine volume so hybrid models are created. Finally, simulation studies are carried out to evaluate the physical parameters for the hybrid processes and to calculate the quantity and quality of brine left.

This simulation study involves solving multiple differential equations simultaneously to study the real-time change in the physical parameters such as permeance, concentration, and pressure drops. Therefore, the equations are solved in Python programming language. And the generated data are stored in Microsoft excel sheets to easily deal with the data.

The simulation studies show that both pervaporation and membrane distillation has good potential to be used in treating seawater reverse osmosis brine. However, pervaporation showed higher permeate water quality than MD with 20% reduction in brine volume per stage. On the contrary, membrane distillation showed higher water flux with 25% reduction in brine volume per stage. Finally, both pervaporation and membrane distillation membranes are capable of treating brine up to 200,000 ppm.

Acknowledgements

First and foremost all thanks due to Allah (The God) for his limitless help and guidance. Then, I would like to thank all the people who made this thesis possible. First, my family for providing me with the warmth and environment. Then, the chemical engineering department primarily my supervisor professor Xianshe Feng for his fantastic approach in leading graduate students. I will not forget to thank my friends and colleagues for their constant help and encouragement. Finally, I'd like to express my sincere appreciation for my employer Saline Water Conversion Corporation (SWCC) and my scholarship administrator Saudi Arabian Cultural Bureau (SACB) in Canada for providing me this amazing opportunity to pursue my Master's degree and funding me generously.

Dedication

This work is dedicated to the people I love, my family.

Table of Contents

List of Figures

List of Tables

List of Symbols

μ	Dynamic viscosity ($Pa \cdot s$)
ϕ	Concentration polarization coefficient (-)
π	Osmotic pressure (Pa)
ρ	Density (kg/m^3)
σ	Osmotic pressure coefficient ($Pa/kg \cdot m^3$)
ξ	Membrane area per unit volume (m^2/m^3 or $1/m$)
A	Water permeation coefficient through the membrane ($kg/m^2 \cdot s \cdot Pa$)
B	Solute transport constant (m/s)
C_B	Solute concentration in the bulk feed solution (kg/m^3 or ppm)
C_b	Solute concentration in the brine or waste concentrated solution (kg/m^3 or ppm)
C_f	Solute concentration in the feed stream (kg/m^3 or ppm)
C_M	Solute concentration at the membrane surface (kg/m^3 or ppm)
C_p	Solute concentration in the permeate or product water (kg/m^3 or ppm)
D	Diffusion coefficient (m^2/s)
D_I	Inner diameter of fiber bundle (m)
d_I	Inner diameter of hollow fiber (m)
D_o	Outer diameter of fiber bundle (m)

d_O	Outer diameter of hollow fiber (m)
d_p	Specific surface diameter (m)
d_s	Inner diameter of hollow fiber submerged in tube sheet (m)
J_s	Solute flux through membrane ($kg/m^2 \cdot s$)
J_v	Solution flux through membrane ($kg/m^2 \cdot s$)
J_W	Water flux through membrane ($kg/m^2 \cdot s$)
k	Mass transfer coefficient (m/s)
L	Effective length of fiber bundle (m)
l	Effective length of hollow fiber (m)
L_s	Length of tube sheet (m)
l_s	Fiber length submerged in tube sheet (m)
N	Number of hollow fibers (-)
P_b	Brine pressure (bars)
P_f	Feed pressure (bars)
P_i	Inlet local permeate pressure (bars)
P_O	Exit local permeate pressure (bars)
P_p	Permeate pressure (bars)
Q	Flow rate (m^3/s)
r	Radial coordinate (n segment)
R_c	Recovery percentage (%)
Re	Reynolds number (-)
S	Membrane surface area (m^2)
Sc	Schmidt number (-)

Sh	Sherwood number (-)
T_b	Brine temperature (°C)
T_f	Feed temperature (°C)
T_p	Permeate temperature (°C)
V	Fluid velocity (m/s)
V_S	Superficial velocity (m/s)
W	Wound number of fibers around the porous feed tube (-)
z	Axial coordinate (m segment)

Chapter 1

Introduction

1.1 Background

Fresh Water availability varies across the world even for the same country or region. This geographical variation in water quantities across the world due to the constant movement of water above and under the ground and in the atmosphere by water cycle and hydrological forces. Besides, the movement of water is heavily impacted by climate change which may turn water abundant areas into water-scarce.

With that being said, there are many areas that are well known to be constantly dry such as desserts and some coastal areas where millions of people are living in. Therefore, the only available solution to provide fresh and potable water is to convert saline water into fresh water using the desalination process. As a result, many countries and regions such as Gulf Countries, many of the Caribbean and Mediterranean Islands, and several municipalities in a large number of countries including the USA and Southern Europe rely on desalination as the main source for potable water.

Desalination processes which are already available in the market on a large scale are multi-stage flashing (MSF), multi-effect distillation (MED) and reverse Osmosis (RO). Although these processes are used extensively, yet they are energy-intensive and not fully sustainable [1]. Not to mention, MSF and MED require more energy compared to RO and this energy is mainly fossil fuel-based [2]. On the other hand, RO can use renewable energy sources such as solar energy to power high-pressure pumps.

Despite the energy challenge for desalination processes, another important challenge is the waste handling i.e. brine from desalination processes is being discharged to the seas

and oceans without treatment [3], whereas brine is around 2.5 times more concentrated than the original feed saline water [1]. In addition, it is bearing other chemicals such as antiscalants (used in MSF and MED) and antifoulants (used in RO) which increase its danger to the aquatic environment. Consequently, zero brine discharge (ZBD) so-called zero liquid discharge (ZLD) is an active research area nowadays with an objective to reuse all the desalination brine and recover its useful minerals such as lithium, strontium and sodium [4]. In the desalination industry, some companies such as Saline Water Conversion Corporation (SWCC) has commissioned its first ZBD desalination plant that uses dual brine concentrator (DBC) process to concentrate brine up to 200,000 ppm and recover lithium and strontium from brine [5].

However, this thesis focuses on the membrane desalination technologies specifically reverse osmosis process which has become the dominant technology for saline water desalination [6]. There are many advantages for the reverse osmosis membranes such as lower energy consumption, less mechanical complexity, and cheaper capital coast [1]. Still, there are many disadvantages for reverse osmosis membranes such as lower lifetime for membranes due to the fouling and scaling and limited mechanical strength [6].

This research focuses on addressing the major adverse impact of desalination processes in general i.e. thermal and membrane technologies that is the brine disposal. Simulation studies are carried out to estimate brine quality and quantity for the reverse osmosis desalination process. Then, case studies are conducted to compare the capabilities of pervaporation and membrane distillation in brine treatment.

1.2 Thesis objectives

The major objectives for this work are:

1. Simulation of hollow fiber saline water reverse osmosis membranes process via a reliable mathematical model.
2. Studying the impact of physical parameters on the operation of hollow fiber saline water reverse osmosis membranes process.
3. Conducting parametric studies to quantify the volume and concentration of brine produced by the above-mentioned process at given conditions and to measure its performance.
4. Carrying out case studies to represent hybrid membrane processes for brine treatment and reuse from saline water reverse osmosis membranes process.

1.3 Methodology

This research is not based on laboratory experiments, rather it is a process design based on simulations. Thus, it is important to find reliable mathematical models to describe each process in use. Therefore, a comprehensive literature review was carried out to find the most accurate and reproducible model to represent the hollow fiber saline water reverse osmosis membranes process.

Also, models for pervaporation and membrane distillation processes are obtained from the literature. All the models are studied and reproduced to ensure their reliability. Once the models are ready, data is obtained either from literature or from industry to run the models. After that, the models are input into computer programs such as Python and Winflows to be solved simultaneously. Finally, the data produced by the models are used to evaluate the performance of the processes under the study and to quantify the volume and concentration of brine after each process.

1.4 Thesis outline

In the first chapter, general background information about water availability and importance are summarized. Then, the thesis objectives, outline, and methodology of conducting this research are explained briefly. The methodology is discussed in more detail in chapters three and four.

The second chapter reviews the literature relevant to this research in the aspects of the impact of brine discharge on aquatic ecosystems and the economic opportunities to utilize brine from desalination processes. Then, the traditional thermal desalination technologies such as multi-stage flashing and multiple effect distillation as well as membrane desalination processes such as pervaporation and membrane distillation are reviewed. Reverse osmosis, the most commonly used desalination technology nowadays, is discussed separately in chapter three.

The third chapter focuses on the engineering aspects of the reverse osmosis desalination process. It includes membranes configurations, materials, and energy recovery techniques. Finally, the most accurate mathematical model for the Hollow fiber reverse osmosis membrane is discussed in more detail.

Chapter four shows the results of parametric studies that are carried out based on the model discussed in the previous chapter. The objective of these parametric studies is to better understand the impact of the physical parameters on the desalination performance

for reverse osmosis membranes. The studied physical parameters include the membrane permeability, membrane area, feed concentration and feed pressure taking into account the pressure drop in the inside the hollow fibers and the concentration polarization.

Chapter five includes a summary of brine utilization case studies. The first case study is the treatment of reverse osmosis brine by pervaporation membranes. And the second case study is the treatment of reverse osmosis brine by membrane distillation. Then, the results of the two case studies are compared. Finally, chapter six provides general conclusions and recommendations related to this research.

Chapter 2

Literature review

2.1 Impact of brine discharge on aquatic ecosystems

The United Nation's 2018 stats show a brine production by desalination industry around the world of 141.5 million m^3/day [7]. And this number is growing annually due to the continual expansion of the desalination industry. However, almost all the brine is discharged back to the water bodies from which the desalination plant's feedwater is originally withdrawn [1, 7]. As a result of brine discharge back to the aquatic ecosystem, and as the density of brine is slightly higher than seawater density, brine flows down towards sea bottom [2, 6]. Thus the concentration of dissolved oxygen in the receiving waters body is reduced [2, 7]. Therefore, high salinity and reduced dissolved oxygen levels can have profound impacts on benthic organisms, which can translate into ecological impacts on all levels of aquatic organisms which are an important part of the human food chain [2, 7].

The other important aspect about the adverse impact of brine on water bodies is the presence of other chemicals such as antiscalants, antifoulants, coagulants, and flocculants [8]. Brine containing these chemicals are normally discharged to water bodies without any treatment [7, 8]. However, most of these chemicals can be recovered but still, there are no feasible commercial processes to do so and this is an active research area currently [8].

2.2 Economic opportunities to utilize brine

Brine reuse, brine mining, or brine refining refers to the process of extracting valuable products from brine. Many salts and metals can be recovered from brine including, magnesium,

gypsum, sodium, calcium, potassium, chlorine, bromine, and lithium [7]. If a feasible and commercial process is found to recover any of these chemicals to be sold separately as another product, this will enhance the economics for the desalination processes.

2.3 Desalination Technologies

Desalination technologies are constantly growing ranging from laboratory scale ideas to commercial technologies which are proven to be economically feasible. This section provides a brief review of commercial desalination technologies. Figure 2.1 [9] shows a list of the most common desalination processes.

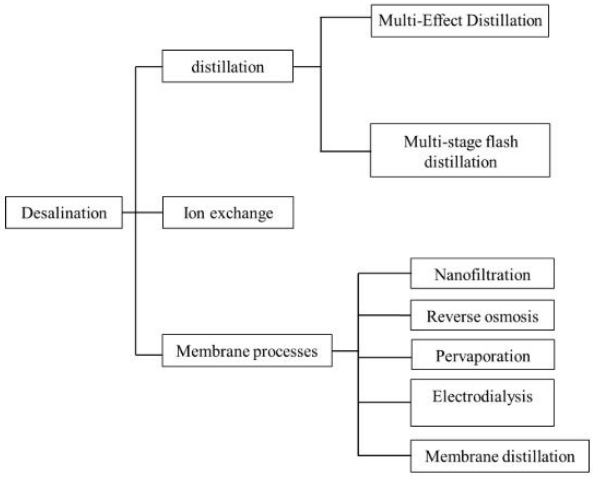

Figure 2.1: List of the most common desalination processes

The use of desalination technologies varies by region in the world for many reasons such as the level of water salinity, average annual temperature and the region income [7]. For example, the Saline Water Conversion Corporation (SWCC) in Saudi Arabia, which is the largest desalination company in the world (as per Guinness World Records 2019), uses thermal processes (mainly MSF and MED) extensively in the eastern region on the Arabian Gulf while SWCC uses membrane processes (mainly reverse osmosis) in the western region on the Red Sea [1]. This variation of the technology used within the same country due to the higher water salinity in the Arabian Gulf (more than 40,000 ppm) where the use of reverse osmosis membranes is more challenging compared to the lower water salinity in the Red Sea (around 35,000 ppm) [10]. With this in mind, the location, size, and type of

technology used in commercial desalination plants (less than 10,000 m^3/day) around the world are illustrated in Figure 2.2 [7].

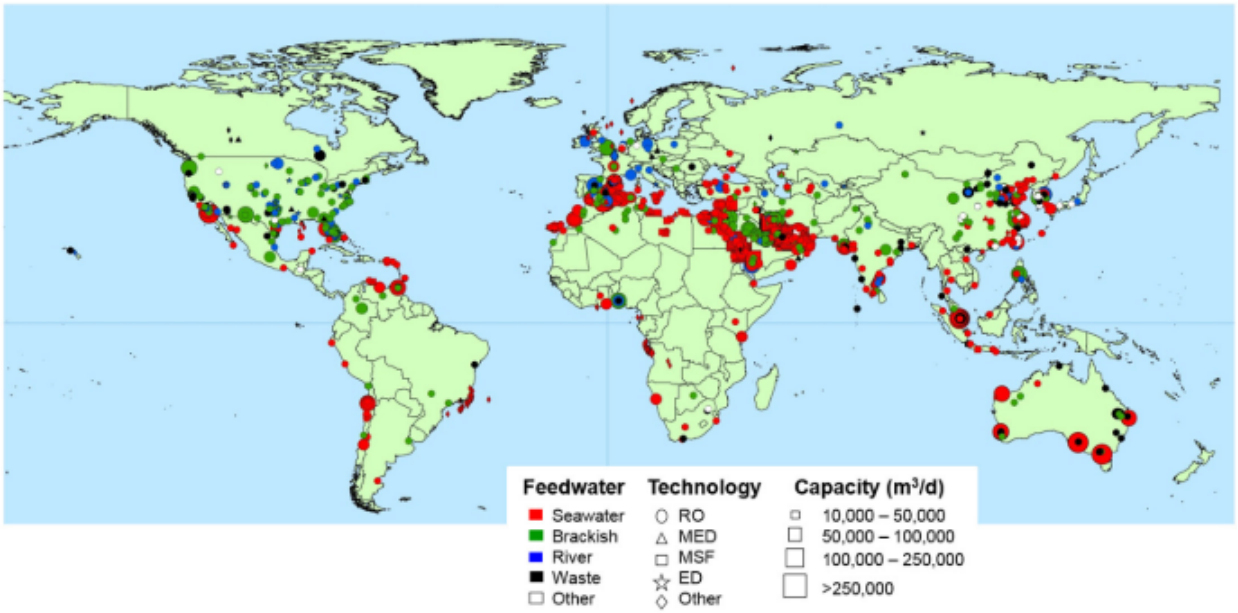

Figure 2.2: Global distribution desalination technology.

Desalination technologies can be classified based on various bases. The following is a list for the commercial desalination processes which are characterized by being mature i.e. well studied and widely implemented in large scales, they are:

1. Multi-stage flashing (MSF)
2. Multi-effect distillation (MED)
3. Reverse osmosis (RO)

The following two sections discuss MSF and MED, briefly while RO is discussed in more detail in chapter 3.

2.3.1 Multi-effect distillation

Multi-effect evaporation (MEE) also called multi-effect distillation (MED), is the oldest thermal desalination process used ever [1]. Yet, it is still in the industry due to the tremendous development this process had so far. In addition, MED requires less heat input compared to MSF due to the application of a higher vacuum [11]. Thus, the maximum temperature in MED is below 70 °C, which minimizes scaling and corrosion compared to MSF [1, 11].

MED is facilitated by a thermal vapor compressor (TVC), and thus it is called MED-TVC, to reduce the steam energy, as shown in Figure 2.3a and 2.3b [1, 12]. The most up-to-date MED units use four effects plus a two-stage condenser in which feed saline water is preheated prior to being fed to the first effect. Also, the condenser is used to reduce the temperature of the discharged brine to ambient temperature by exchanging heat between feed and brine. An example of such MED units is the MED unit commissioned in 2017 by SWCC in Saudi Arabia with a production capacity of 91,200 m^3/day which is the largest in the world.

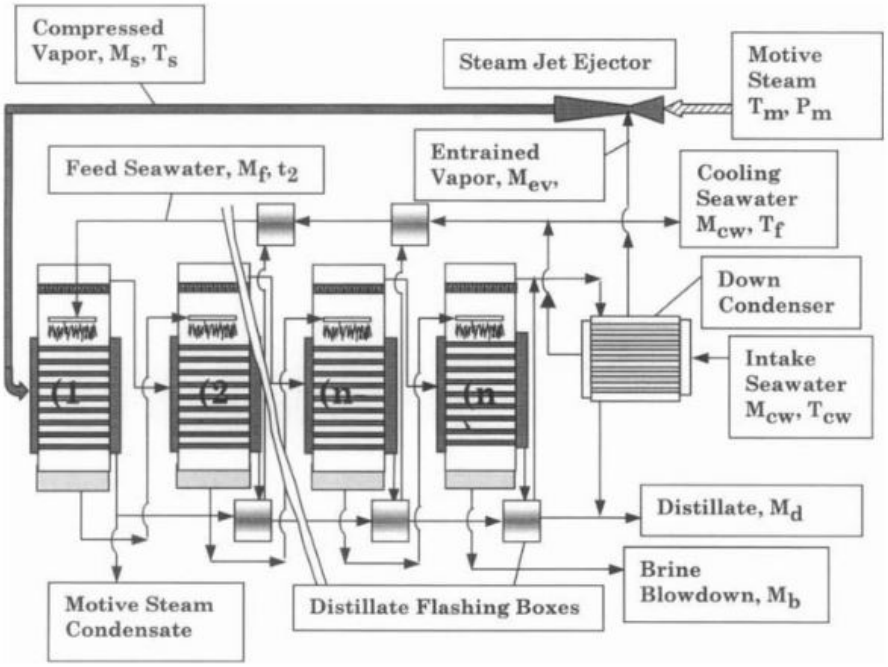

(a) MED process flow diagram 1 [1]

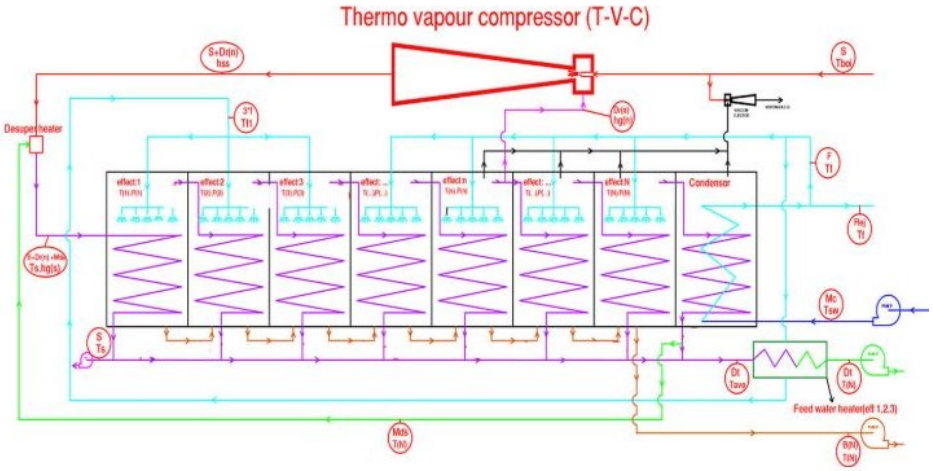

(b) MED process flow diagram 2 [11]

Figure 2.3: Illustration for MED process

Operation of MED

The principle for MED-TVC is summarized as follows [1]:

- Steam from boilers (so-called motive steam) is compressed in the TVC to lower energy in order to maintain its temperature below 70 °C. Then, it enters the first effect through a set of thin and narrow tubes called the evaporator tubes bundle (ETB).
- At the same time, the preheated feed saline water is fed to the first effect and sprayed over the ETB from the top. Thus, the evaporation takes place on the outer surface of each tube in the ETB.
- The generated vapor is fed to the ETB of the next effect, while the condensed water inside the ETB flows out of the effects as product water. The same sequence repeats in each effect.
- Finally, brine generated in each effect flows to the condenser and it is used to preheat feed saline water before it gets discharged as a waste.

2.3.2 Multi-stage flashing

Similar to MED, multi-stage flash desalination (so-called multi-stage flashing) is one of the oldest, still in the use, thermal desalination technology. It had been developed as an upgrade to the MED process by making the evaporation takes place on the surface of bulk saline water instead of the surface of evaporator tubes as in MED [1]. This feature allows more steam to be generated which increases the production capacity per unit in MSF [12]. However, this requires more heat input which makes MSF less desirable nowadays especially after emerging reverse osmosis desalination membranes.

The general MSF process flow diagram is shown in 2.4a. It operates on the evaporation-condensation principle where a huge amount of heat is required to evaporate saline water and then the generated steam thermally contacts with cold feedwater in a series of connected and declining pressure and temperature chambers (stages) that are installed into one huge body (called the evaporator) as illustrated in Figure 2.4b [1]. MSF evaporators can contain up to 24 consecutive stages in large desalination plants [1]. Each stage is maintained at a specific temperature and vacuum by the incoming brine and the steam ejectors at the top of the evaporator [12].

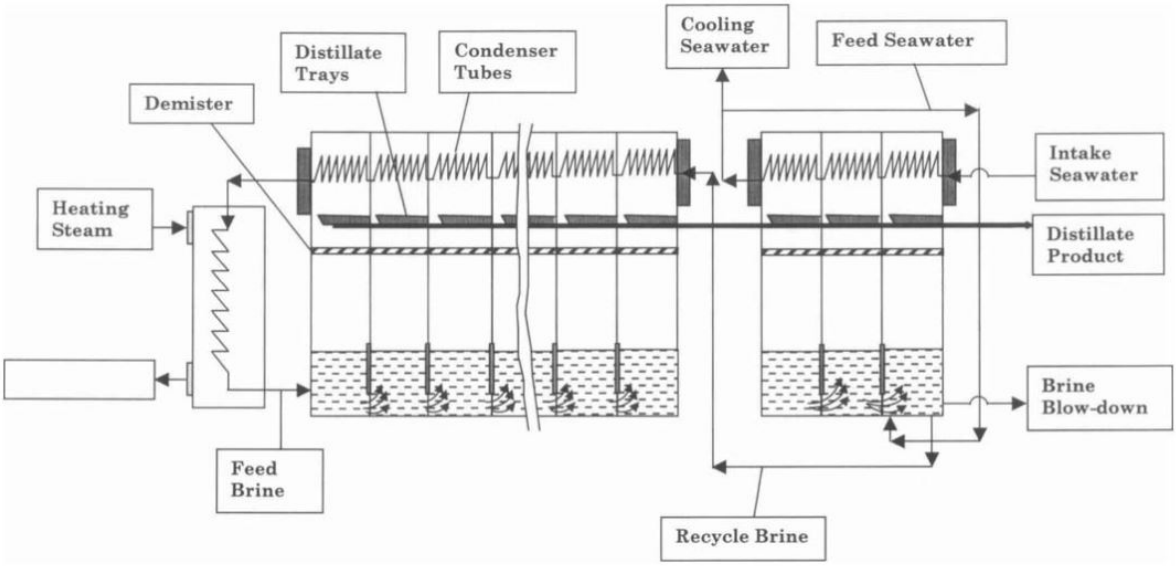

(a) MSF process flow diagram [1]

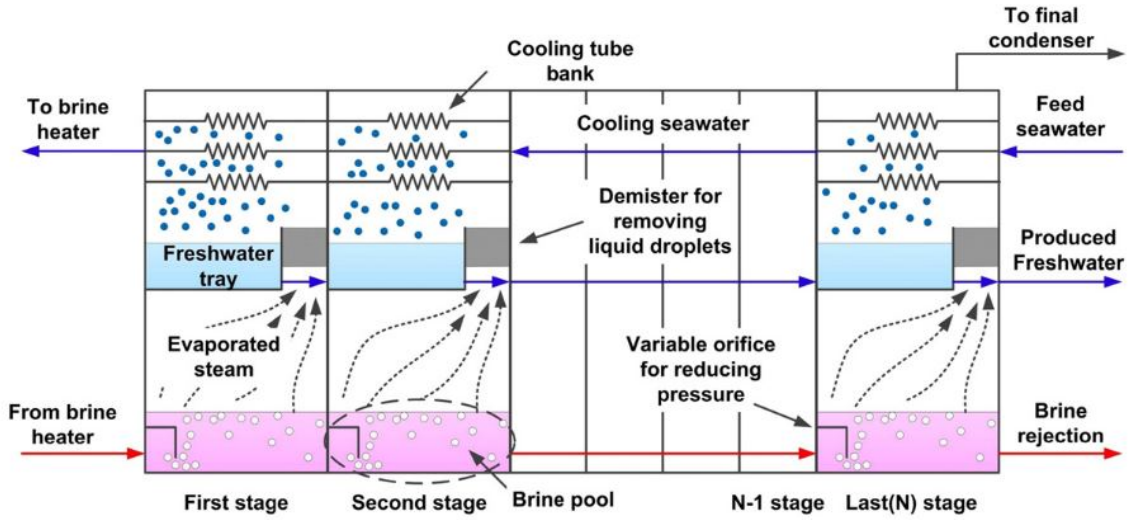

(b) MSF chambers [12]

Figure 2.4: Illustration for MSF process

Operation of MSF

The operation of MSF is well known as the brine circulation process which can be summarized in the following [1]:

- Cold saline water enters the top of the last chamber (stage) through a bundle of a large number of thin tubes (called condenser tubes) where it is preheated with the brine flowing into the bottom of the stage but in opposite direction.
- Temperature of preheated saline water is gradually increased in each stage until it reaches the brine heater which exchanges the heat between incoming steam from boilers and preheated feed saline water to maintain the temperature around 130 °C. This temperature is called top brine temperature (TBT) which is an important factor for the design and operation of MSF.
- The fully heated feed saline water enters the bottom of the first stage where part of it evaporates and the other part moves to the next stage. The same flashing process takes place in each subsequent stage; this is why MSF is given this name.
- Once the flashing happens, steam moves up though the demisters to remove mist (tiny water droplets) that might be dragged with the generated steam in the chamber. After that, the steam condenses around the condenser tubes, the condensed water is called distillate and it is collected in the distillate trays.
- Finally at the last stage, the accumulated distillate is collected as product water while part of the accumulated brine is recycled to the evaporator to recover heat and the rest is discharged as a waste.

Despite the high capital and operational costs, the major advantages of MSF can be summarized in the following points:

1. Process reliability and withstanding harsh conditions.
2. Desalinating higher salinity water.
3. Higher purity distillate.
4. Longer equipment lifetime.

Another category is the emerging membrane desalination technologies which are still under development. Therefore, they are not applied on a large scale [6]. For this research, the following processes are not meant to be used for desalination independently, rather they are used to produce water by further processing of brine from the above-mentioned processes. These technologies are:

1. Pervaporation (PV)
2. Membrane distillation (MD)
3. Forward osmosis (FO)

The following sections review the above-listed membrane technologies which could be utilized to treat reverse osmosis membranes brine.

2.3.3 Pervaporation

This section briefly reviews the pervaporation (PV) process for treating high salinity water.

The track for the modern studies on the PV process gets back to the 1950s by Binning and coworkers [6]. PV uses vapor pressure difference between the feed and product streams to separate fluids by supplying low-grade heat to the liquid feed stream and applying a constant vacuum on the product stream [6, 9]. Due to the phase change of feed stream from liquid to vapor, the permeated components are collected as vapor. Therefore, a condenser is used only if the product is needed to be collected in a liquid phase, as shown in Figure 2.5 [13].

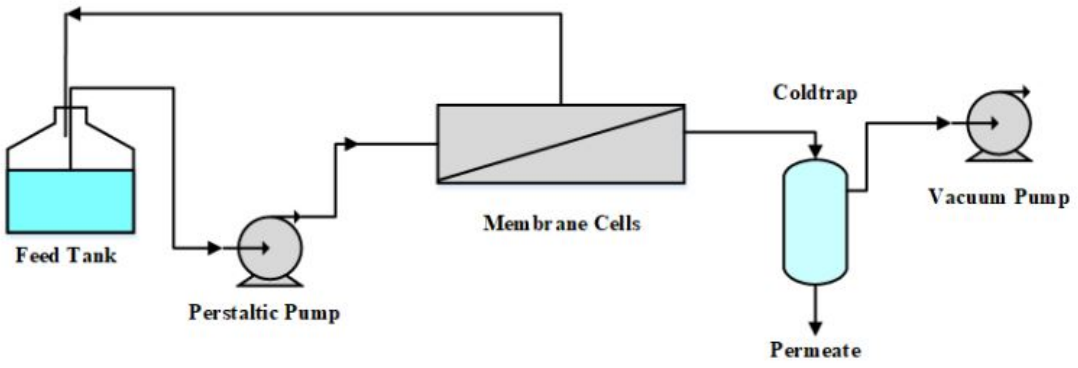

Figure 2.5: Pervaporation process flow diagram.

Dense and selective membranes are used to facilitate the permeation of the desired components and reject the others [14]. The separation capability is determined by the selectivity of the membranes which is a function of solubility and diffusivity of permeating components through specific membrane material [9, 15].

Materials for Pervaporation

Many materials are used for making pervaporation membranes such as sulfonated polyethylene, cellulose triacetate, graphene oxide/polyacrylonitrile and poly(ether block amide) (PEBA) [9, 16–18]. The data for this research is based on PEBA membranes with a general chemical structure shown in Figure 2.6 [19]. PEBA is stable between -40 and 80 °C with resistance to many chemicals and corrosion which make it a good polymer to be used in PV membranes for treating high saline water [9].

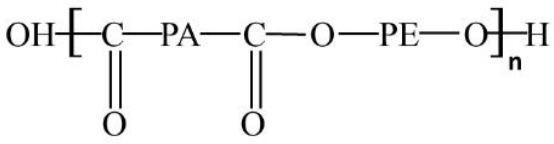

Figure 2.6: Chemical structure for PEBA.

Pervaporation performance analysis

The discussion in this section is limited only for the important performance parameters for the PV process such as water flux and separation factor.

The flux in PV membranes is defined as [6]:

$$J_i = \frac{D_i K_i^G \left(p_{i_o} - p_{i_\ell}\right)}{\ell} = \frac{P_i^G}{\ell}\left(p_{i_o} - p_{i_\ell}\right) \tag{2.1}$$

where J_i is the flux of component i through a PV membrane, D_i is the diffusivity for component i through the membrane, K_i^G and K_i^L are membrane sorption constants in vapor and liquid phases, respectively, p_{i_o} and p_{i_i} are partial vapor pressures before and after the PV membrane, respectively, ℓ is the membrane thickness, and $P_i^G = D_i \cdot K_i^G$ is the membrane permeability constant.

An indication for membrane selectivity in in PV is given by the separation factor β_{pervap} which is equivalent to salt rejection in RO and it is given by [6, 20]:

$$\beta_{\text{pervap}} = \frac{c_{i_\ell}/c_{j_\ell}}{c_{i_o}/c_{j_o}} = \frac{p_{i_e}/p_{j_\ell}}{c_{i_o}/c_{j_o}} \tag{2.2}$$

where c_{i_ℓ}/c_{j_ℓ} is the concentration ratio of component i and j in the permeate side and c_{i_o}/c_{j_o} is the concentration ratio in feed side. Since the salt concentration of permeate is very low, vapor pressure can be used to determine the selectivity.

2.3.4 Membrane Distillation

This section briefly reviews the membrane distillation (MD) process focusing on its ability for treating high salinity water.

Similar to pervaporation, membrane distillation is a thermally driven process with a phase change. However, the types of the membrane and the mass transfer mechanisms different. [21]. In MD, porous hydrophobic membranes are used to separate water from salts based on transmembrane water pressure difference, as illustrated in Figure 2.7 [6, 15, 21].

Configurations for MD membranes

There are four main configurations for MD membranes [15, 21]:

1. Direct Contact Membrane Distillation (DCMD)
2. Air Gap Membrane Distillation (AGMD)
3. Sweeping Gas Membrane Distillation (SGMD)
4. Vacuum Membrane Distillation (VMD)

The conceptual diagrams in Figure 2.8 [21] compare the major types of MD. However, DCMD is the most studied configuration due to its simplicity [22].

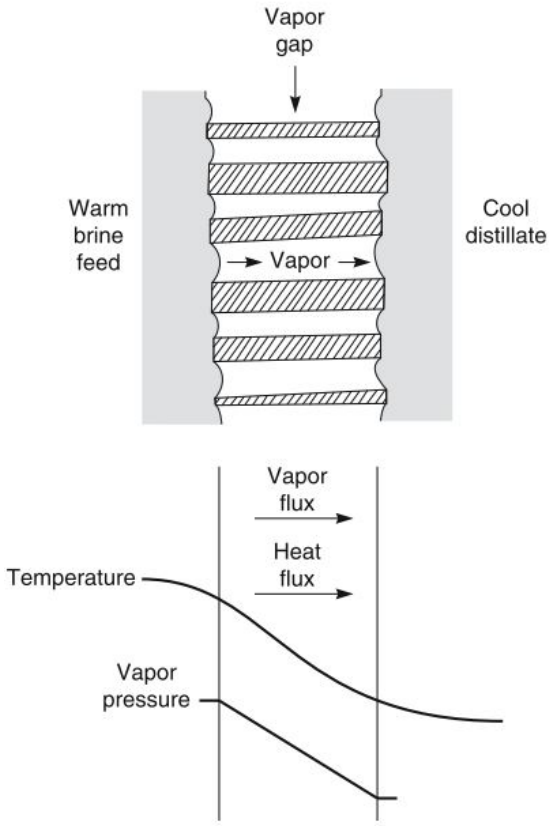

Figure 2.7: MD temperature and water vapor pressure gradients.

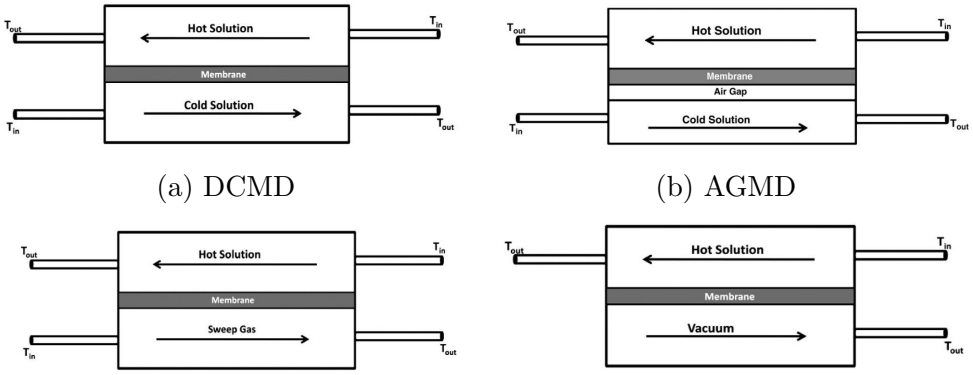

(a) DCMD (b) AGMD

(c) SGMD (d) VMD

Figure 2.8: Types of MD configurations

Materials for MD membranes

For a material to be used in the MD process, the pores of the membrane should not be wetted by liquid water. Therefore, the feed pressure should not exceed the liquid entry pressure which is an important parameter in the design and operation of the MD process. However, the most common materials used in MD membranes are polypropylene (PP), polyvinylidene fluoride (PVDF) and polyethylene (PE) [22].

Performance analysis for MD membranes

Water flux through MD membrane depends on the configuration used (i.e. DCMD, AGMD, SGMD or VMD). For the simplest configuration (DCMD), transmembrane water flux can be expressed as [22]:

$$J_w = B_w \Delta p_w \tag{2.3}$$

where B_w is the membrane permeability coefficient and Δp_w is the partial vapor pressure difference of water across the membrane.

Separation factor (so-called membrane rejection) for MD processes is given by:

$$\alpha = \left(1 - \frac{C_p}{C_f}\right) 100 \tag{2.4}$$

where C_p and C_f are salt concentrations in permeate and feed, respectively.

Treating RO brine by MD process

Many studies in recent years are conducted on the treatment of reverse osmosis membranes brines using MD processes, mainly DCMD, due to its simplicity [2]. Furthermore, another major attraction towards the MD process is the high recoveries that can be achieved regardless of the feed salt concentration since the vapor pressure for the brine feed is not strongly dependent on the osmotic pressure [22]. This is because MD is a heat-driven process and the membranes used are porous and hydrophobic [15, 21].

2.3.5 Forward Osmosis

Direct Osmosis (DO) or Forward Osmosis (FO) is the original process from which reverse osmosis is derived. FO utilizes the osmosis forces generated between solutions of unequal concentrations of a specific component separated by a semipermeable membrane [23]. In such conditions, water will flow from low to high concentration solutions due to the chemical potential gradient between the two solutions on each of the membrane sides [24]. Osmosis is a naturally occurring physical process through which water and nutrients move from the ground to the top of trees [25]. In industry, a draw solution (highly concentrated) is used to drive the FO process. For example, brine from seawater can be used as a draw solution when diluting seawater by wastewater in which water moves from wastewater to seawater [23]. This can reduce the scaling and fouling of in seawater reverse osmosis process [25].

The type of membranes used in FO are typically dense cellulose triacetate (CTA) supported by polyester layers as per Figure 2.9 [26] [25].

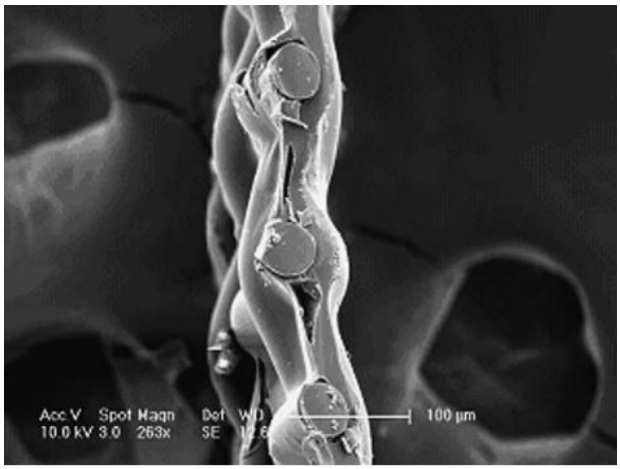

Figure 2.9: CTA membranes supported by polyester used in FO desalination

FO can be used for desalination directly if an economical and a practical draw solution is available [25]. For example, Figure 2.10 [27] shows a lab scale FO desalination process in which a mixture of ammonia (NH_3) and carbon dioxide (CO_2) were used as a draw solution [26].

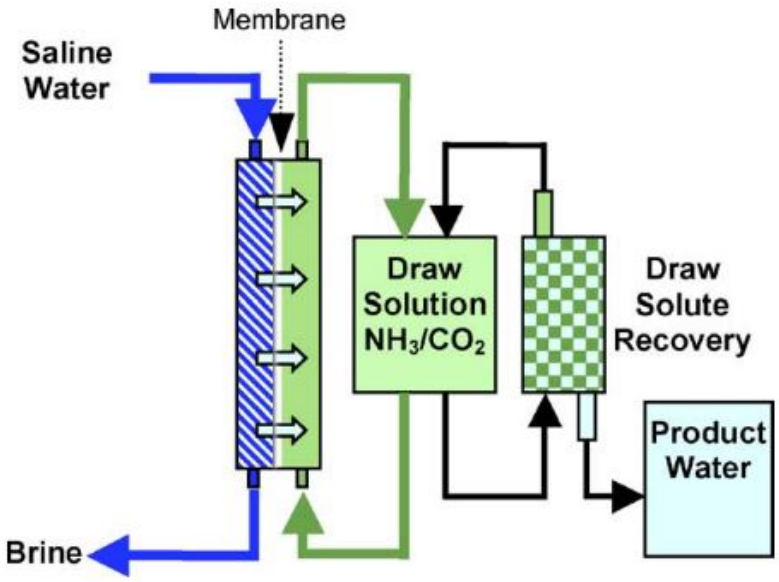

Figure 2.10: FO desalination using NH_3−CO_2 draw solution.

Chapter 3

Reverse osmosis process engineering

This chapter covers general engineering aspects of the reverse osmosis desalination process. The most common materials used to manufacture seawater reverse osmosis membranes, design configurations, and energy recovery devices are discussed. Finally, the major challenges facing seawater reverse osmosis membranes and the mathematical models used to describe the process are covered focusing on models for hollow fiber seawater reverse osmosis membranes.

3.1 Configurations for reverse osmosis desalination membranes

The following are the three main design configurations popular in manufacturing reverse osmosis membranes:

1. Flat sheet configuration.
2. Spiral wound configuration.
3. Hollow fiber configuration.

3.1.1 Flat sheet membranes configuration

Flat sheet is the basic membrane configuration where pressure is applied to move water across a flat sheet of semi-permeable dense membrane. However, flat sheet membranes are usually used in the research stages for developing and testing new membranes. It is rarely applied in the desalination industry for commercial applications due to its low area-to-volume ratio (so-called packing density) which quantifies the membrane area can each module hold [28]. This means more footprint for the plant or facility for the installation of flat sheet membranes to produce the same quantity of water compared to spiral wound and hollow fiber modules [6].

Plate and frame design configuration is not widely used in the desalination industry [1]. The idea for designing plate and frame membranes is adopted from plate and frame heat exchangers, where the flat sheet of the membrane is cut into small pieces and stacked vertically or horizontally relative to each other, separated by spacers and contained into a frame [2, 6, 28]. A schematic diagram for plate and frame membrane modules is shown in figure 3.1 [28]. Regardless of how easy and versatile to operate plate and frame membranes, high hydraulic pressure must be avoided due to the lack of physical support among the membrane sheets in the plate and frame membrane modules [29].

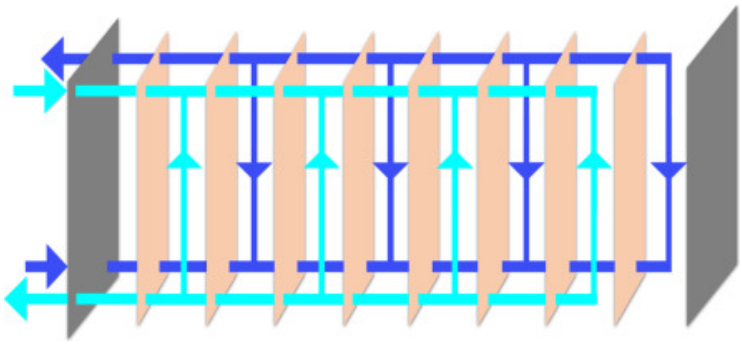

Figure 3.1: Schematic illustration of plate and frame configuration.

3.1.2 Spiral wound membranes configuration

Spiral wound configuration was developed after the flat sheet membranes and it is commonly used in the desalination industry [30]. As shown in Figure 3.2 [30], spiral wound membranes consist of flat sheet membrane leaves, and the spacers are added alternatively among the sheets to form a leaf assembly. After that, the leaves are wound around a central perforated tube which distributes water to the membrane. Finally, all the pieces are contained into a pressure vessel [1, 2].

In spiral wound reverse osmosis membranes, feed water flows axially along the module through feed spacers. Therefore, this configuration can handle high pressure due to the use of spacers successively after each membrane leaf [30]. Although the packing density in spiral-wound modules is higher than the plate and frame modules, still it is not the best packing density, which translates to a considerable footprint for spiral wound modules.

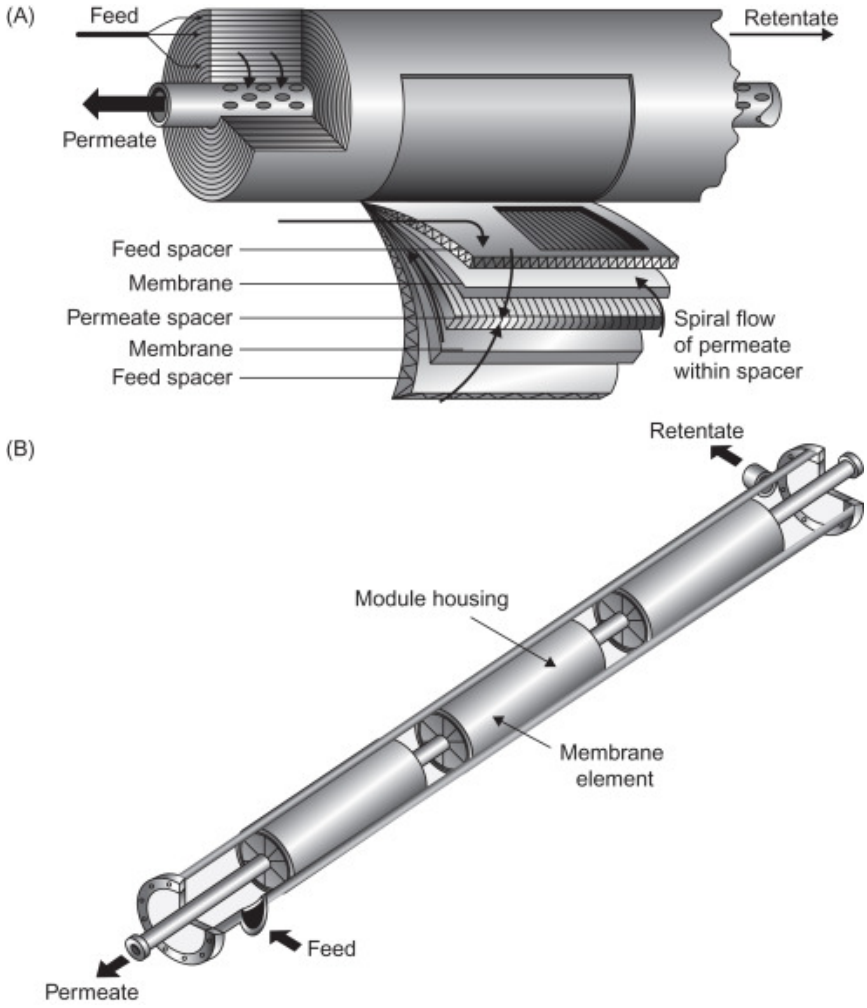

Figure 3.2: Spiral-wound membranes: (A) element configuration and (B) module construction.

3.1.3 Hollow fiber membranes configuration

Hollow fiber is the latest configuration used in reverse osmosis desalination. It has the maximum area-to-volume ratio (packing density) among all the modules. As illustrated in Figure 3.3 [31], hollow fiber modules consist of tiny membrane tubes with an inner diameter in the range of 42 - 77 μm [1, 32]. These tiny tubes are cross-wound around a perforated central tube and contained in a pressure vessel. Thus, each pressure vessel contains millions on hollow fibers and this is why the packing density is the highest in hollow fiber modules compared to the plate and frame and spiral wound modules [31].

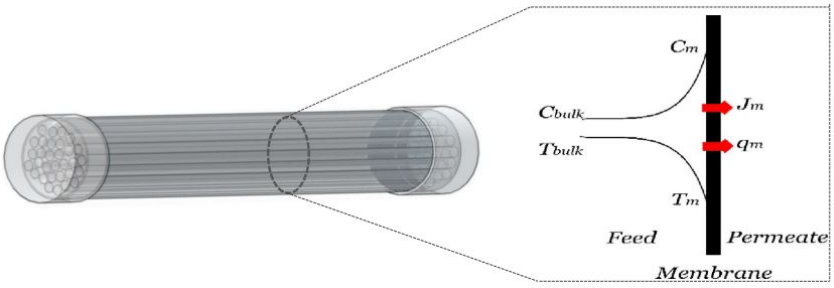

Figure 3.3: Schamic diagram for a general hollow fiber module.

3.2 Materials for reverse osmosis desalination membranes

The most commonly used materials to manufacture reverse osmosis membranes are cellulose acetate and polyamides, which are discussed briefly in the following sections:

3.2.1 Cellulose acetate

Cellulose acetate, as shown in Figure 3.4 [6], is the first material used to develop reverse osmosis membranes in the early 1960s by Loeb and Sourirajan [6]. It is a blend of diacetate and triacetate films on a support layer [1, 6]. Cellulose acetate membranes are prepared by the thin film casting process and they are asymmetric with a dense and thin surface layer that is responsible for the membrane selectivity [1]. The thin membrane surface layer is placed on microporous support materials to give it mechanical strength [6].

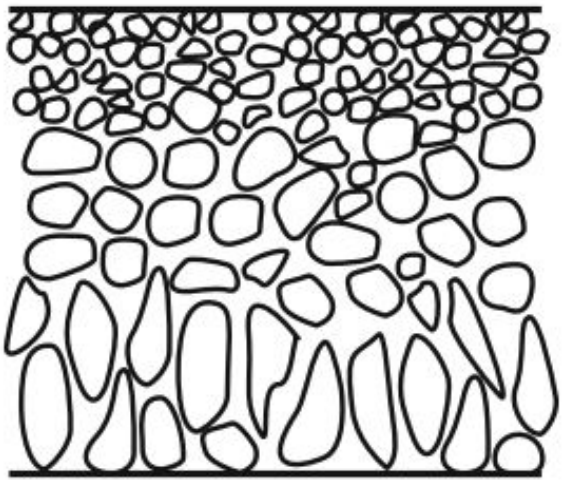

Figure 3.4: Schematic diagram for cellulose acetate membranes.

3.2.2 Polyamides

Thin-film composite membranes are another class of reverse osmosis membranes. Thin-film composite membranes provide high water flux and salt rejection compared to asymmetric cellulose acetate membranes, but it suffers from attacks of free chlorine which deteriorates polyamide structure [1, 6, 33]. Therefore, a common practice developed in the desalination industry is that, the thin film composite membranes are used in the second pass after the majority of free chlorine in water is separated by the first pass with asymmetric cellulose acetate membranes.

In terms of chemical structure, thin-film composite membranes are a thin and selective film of polyamide usually in 20 - 200 nm thick deposited by interfacial polymerization process over a porous polysulfone and polyester support layers (so-called substrates), as shown in Figure 3.5 [6]. They are prepared by the interfacial polymerization reaction as in Figure 3.6 [24, 33–35].

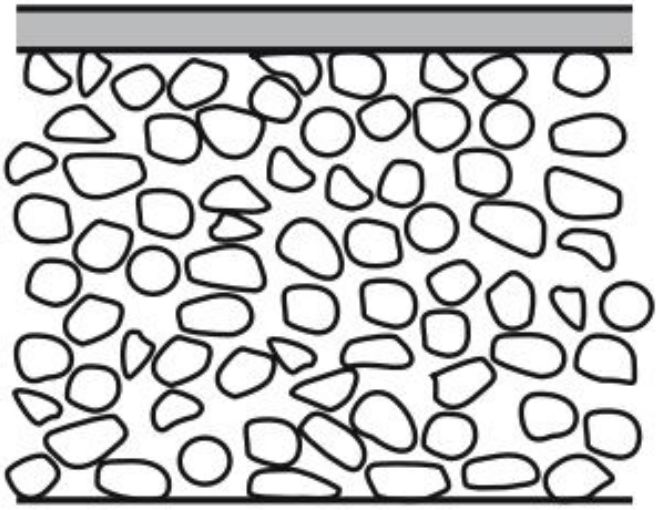

Figure 3.5: Schematic diagram for thin film composite membranes.

The reaction is shown in Figure 3.6 [33] is the most commonly used reaction in production of thin-film composites reverse osmosis membranes, which represents only a framework for such reaction i.e. the monomer type and concentration can be changed in order to optimize the membrane performance for specific application or to control the production cost [33].

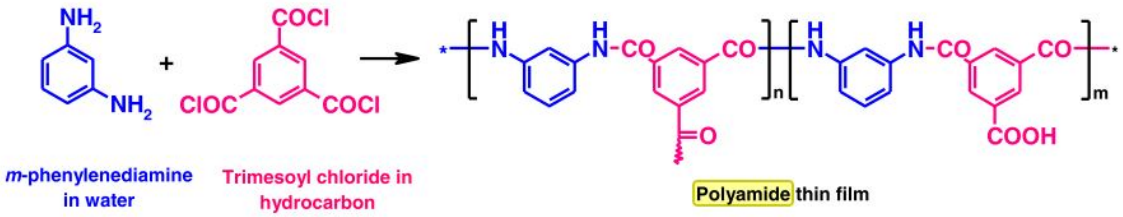

Figure 3.6: Interfacial polymerization for thin film composite membranes.

Thin-film composite reverse osmosis membranes are an active research area currently due to its capability to handle chemical modifications, which include nano additives such as zeolite, nano-tubes, and graphene to change surface morphology. This may enhance water flux and salt rejection as well as fouling resistance and specific elements rejection [36].

3.3 Energy recovery for reverse osmosis

3.3.1 Pressure exchangers

Although the temperature impact in the seawater reverse osmosis process is limited, i.e., the process is operated isothermally, the impact of pressure on process economics is very important [1, 6]. Operating feed pressure is directly related to the water flux as expressed by Eq. 3.1. Operating pressure in seawater reverse osmosis membranes processes is supplied by high-pressure pumps and can reach 80 bar based on saline feed water concentration [1]. The total pressure drop in the membrane module can be as low as 2 bars based on the operating conditions and the membrane lifespan [1, 6, 37]. This means more than 90 % of the operating pressure is lost if not recovered. Therefore, the idea of pressure exchangers (PXs) had been exploited. PXs use booster pumps to convey pressure from reject brine stream to feed saline steam without physically contact the two streams. Thus, high-pressure pumps are used only at the beginning of the operation cycle and intermittently when the pressure is lost from the RO process [37].

3.3.2 Pressure retarded osmosis

Pressure retarded osmosis (PRO) is a membrane process aimed mainly to recover waste energy from the RO process. Both PXs and PRO can be used together to recover energy from RO as illustrated in Figure 3.7 [38] where PXs are used to recover hydraulic pressure while PRO is used to recover osmotic energy [38].

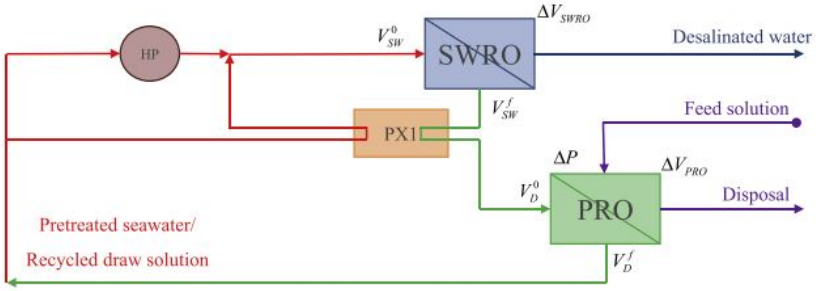

Figure 3.7: The use of PRO and PXs to recover energy in reverse osmosis desalination process.

3.4 Mathematical models for hollow fiber reverse osmosis membranes

There are various analytical models for hollow fiber reverse osmosis membrane modules since the 1970s, which vary based on the complexity of the preset assumptions. However, the most realistic models are the ones with minimal assumptions. Simple models assume negligible concentration polarization (CP) and pressure drop inside the fibers (dP-fiber) [39]. Thus, model complexity increases as one or both of the previous parameters are taken into account. Based on the literature review in this research, the Friction-Concentration Polarization model (FCP model) was found to be the most accurate model to describe hollow fiber reverse osmosis membranes as it accounts for both CP and dP-fiber[32].

The FCP-Model assumptions:

1. Flow in the hollow fiber reverse osmosis membranes is based on the solution-diffusion model.
2. No change in temperature; isothermal conditions.

3.4.1 FCP-Modelling

According to the solution diffusion model [6, 32], water and salt fluxes are defined as:

Water flux:

$$J_W = A(\Delta P - \Delta\pi) \tag{3.1}$$

Salt flux:

$$J_{\mathrm{s}} = B\Delta C \tag{3.2}$$

Concentration polarization results from gradual accumulations of the non-permeating salts close to the membrane surface and is defined as:

$$\frac{C_{\mathrm{M}} - C_{\mathrm{P}}}{C_{\mathrm{B}\text{-}} C_{\mathrm{P}}} = \exp\left(J_{\mathrm{V}}/k\right) \tag{3.3}$$

Total permeation flux through the membrane consists of salt and water fluxes:

$$J_{\mathrm{V}} = \frac{J_{\mathrm{W}} + J_{\mathrm{S}}}{\rho_{\mathrm{P}}} \tag{3.4}$$

Permeate salt concentration can be calculated from total permeation flux equation:

$$C_{\mathrm{P}} = J_{\mathrm{S}}/J_{\mathrm{V}} \tag{3.5}$$

The mass transfer coefficient (k) can be determined using semi-empirical correlations:

$$Sh = kd_{\mathrm{O}}/D = Sh(Re, Sc) \tag{3.6}$$

Since water flowing inside the fiber is incompressible (no change in its density along the fiber) as well as it is Newtonian and laminar flow is assumed, and based on the similarity in the geometry of the hollow fibers to the cylindrical pipes, the Hagen-Poiseuille equation can be used to calculate the pressure drop inside the fibers:

$$\frac{\mathrm{d}P}{\mathrm{d}z} = \frac{128\mu \mathrm{Q}_{\mathrm{P}}}{\pi d_{\mathrm{I}}^4} \tag{3.7}$$

The hollow fibers are held inside a pressure vessel in the form of a U-shaped bundle of millions of fibers. Thus, based on the similarity in the geometry of the pressure vessel to the packed bed columns, the pressure drop for the bundle is quantified by the Ergun equation:

$$\frac{\mathrm{d}P}{\mathrm{d}r} = \frac{150\sigma^2\mu}{(1-\sigma)^3 d_{\mathrm{P}}^2} V_{\mathrm{S}} + \frac{1.75\sigma\rho}{(1-\sigma)^3 d_{\mathrm{P}}} V_{\mathrm{S}}^2 \tag{3.8}$$

The reason for choosing the Hagen-Poiseuille equation for the pressure drop inside the fiber is because the coordinates is considered to be linear as the fiber is divided into infinitesimal segments. Therefore, the local pressure is calculated for each segment, then

the total pressure is summed up by integration over the fiber length. The Ergun equation is used based on the circular configuration of the fiber bundle.

The material balance within a fiber bore can be written as:

$$\frac{dQ_P}{dz} = \pi d_O J_V, \quad l_S \leqslant z \leqslant l_S + l \tag{3.9}$$

While the material balance within a fiber bundle is written as:

$$\frac{\mathrm{d}Q_\mathrm{B}}{\mathrm{d}r} = -2\pi r L(1-\sigma)J_\mathrm{V}\zeta \tag{3.10}$$

By adding solute concentrations, the material balance within a fiber bundle can be rewritten as:

$$\frac{\mathrm{d}Q_\mathrm{B}C_\mathrm{B}}{\mathrm{d}r} = -2\pi r L(1-\sigma)J_\mathrm{V}C_\mathrm{P}\zeta \tag{3.11}$$

where for both 3.10 and 3.11:

$$\frac{D_1}{2} \leqslant r \leqslant \frac{D_0}{2} \tag{3.12}$$

By taking the derivative of Eq. 3.7 and substituting it into Eq. 3.9, the following second order differential equation is produced:

$$\frac{\mathrm{d}^2P}{\mathrm{d}z^2} = \frac{128\mu}{d_1^4} d_\mathrm{O} J_\mathrm{v} \tag{3.13}$$

With the following boundary conditions:

$$P = P_\mathrm{O} \quad \text{at } z = 0 \tag{3.14}$$

$$P = P_\mathrm{O} + \left.\frac{\mathrm{d}P}{\mathrm{d}z}\right|_{z=l_s} \cdot l_\mathrm{s} \quad \text{at } z = l_\mathrm{S} \tag{3.15}$$

$$\frac{\mathrm{d}P}{\mathrm{d}z} = 0 \quad \text{at } z = l_\mathrm{S} + l \tag{3.16}$$

For almost all hollow fiber reverse osmosis modules, the fibers are wound spirally around a porous core tube, so the membrane area is expressed as:

$$\mathrm{d}S = \pi D_\mathrm{o} l \mathrm{d}N \tag{3.17}$$

where,

$$l = \sqrt{L^2 + 4(\pi r W)^2} \tag{3.18}$$

3.4.2 Solving FCP Model

In this research, the FCP model is reproduced to make sure of its reliability. Then, it is used to test seawater reverse osmosis membranes performance. The most important parameters to be determined using the FCP model are water productivity and salt rejection. All the equations in the FCP model have to be solved simultaneously. Thus, a finite difference method (FDM) was used to solve the model equations numerically with the help of Python and MATLAB [32].

In FDM, the fiber is projected into Cartesian coordinates where the length is divided into infinitesimally small segments along the x-axis denoted as m. The same division is done for the fiber height but in the y-axis, denoted as n. Therefore, the membrane is divided into tiny local areas ($m \times n$) in which the performance parameters are calculated then integrated over the total surface area of the membrane.

The FCP model can be re-written in a finite difference form to be input easily in the computer as follows [32]:

Osmotic pressure is related to the solute concentration by the following equation:

$$\Pi = \alpha C \tag{3.19}$$

Concentration polarization coefficient can be defined as:

$$\Phi = \frac{C_M - C_P}{C_B - P_P} \tag{3.20}$$

With the help of equations 3.19 and 3.20, water and salts fluxes can be written as follows:

$$\begin{aligned} J_{\mathrm{W}} &= A\left[\left(P_{\mathrm{B}} - P_{\mathrm{P}}\right) - \left(\Pi_{\mathrm{M}} - \Pi_{\mathrm{P}}\right)\right] \\ &= A\left[\left(P_{\mathrm{B}} - P_{\mathrm{P}}\right) - \alpha\Phi\left(C_{\mathrm{B}} - C_{\mathrm{P}}\right)\right] \end{aligned} \tag{3.21}$$

$$J_{\mathrm{S}} = B\left(C_{\mathrm{M}} - C_{\mathrm{P}}\right) = B\Phi\left(C_{\mathrm{B}} - C_{\mathrm{P}}\right) \tag{3.22}$$

The permeate water flux through the axial segment of the fiber (dz) is given by:

$$\begin{aligned} J_{\mathrm{V}ij} =& \frac{J_{\mathrm{W}ij} + J_{\mathrm{S}ij}}{\rho_{\mathrm{P}ij}} \\ =& A\left[\left(P_{\mathrm{B}ij} - P_{\mathrm{P}ij}\right) \quad -(\alpha A - \mathrm{B})\Phi_{ij}\left(C_{\mathrm{B}ij} - C_{\mathrm{P}ij}\right)\right]/\rho_{\mathrm{P}ij} \end{aligned} \tag{3.23}$$

Therefore, the local concentration polarization factor can be written as:

$$\Phi_{ij} = \exp\left(J_{\mathrm{Vij}}/k_{ij}\right) \tag{3.24}$$

While the local mass transfer coefficient is derived from equation 3.6 as:

$$k_{ij} = 0.048\left(\frac{D_{ij}}{d_{\mathrm{O}}}\right)\left(\frac{d_{\mathrm{O}}V_{\mathrm{B}ij}\rho_{\mathrm{B}ij}}{\mu_{\mathrm{B}ij}}\right)^{0.6}\left(\frac{\mu_{\mathrm{B}ij}}{\rho_{\mathrm{B}i}D_{ij}}\right)^{1/3} \tag{3.25}$$

The solute permeation parameter is derived in the form of quadratic equation from equations 3.5, 3.22 and 3.23 as:

$$C_{\mathrm{P}ij} = \left(-a_1 + \sqrt{a_1^2 - 4a_0a_2}\right)/2a_2 \tag{3.26}$$

where

$$\begin{aligned} a_0 =& -B\Phi_i C_{\mathrm{B}i}\rho_{\mathrm{Pij}} \\ a_1 =& A\left(P_{\mathrm{B}ij} - P_{\mathrm{Pij}}\right) \\ & -(\alpha A - B)\Phi_{ij}C_{\mathrm{Bij}} + B\Phi_{ij}\rho_{\mathrm{Pij}} \\ a_2 =& (\alpha A - B)\Phi_{ij} \end{aligned} \tag{3.27}$$

Integrating Eq. 3.13 leads to local permeate pressure which is written in a finite difference form as:

$$P_{\mathrm{P}ij} - P_{\mathrm{P}ij-1} = \frac{128\mu_{\mathrm{P}ij}\Delta z^2 d_{\mathrm{O}}}{d_{\mathrm{I}}^4}\sum_{j=j}^{n} J_{\mathrm{V}_{ij}} \tag{3.28}$$

As moving along the fiber length, the permeate pressure inside the fiber segments converges to the exiting pressure at the fiber opening, and this is represented by the following equation:

$$P_{\mathrm{Pi1}} - P_{\mathrm{PiO}} = \frac{128\mu_{\mathrm{Pii}}l_{\mathrm{S}}\Delta z d_{\mathrm{O}}}{d_{\mathrm{S}}^4}\sum_{j=1}^{n} J_{\mathrm{V}ij} \tag{3.29}$$

where d_{S} and l_{S} are the inner diameter and the length of the hollow fiber, respectively.

The axial pressure outside the fiber bundle (so-called the feed pressure) is derived from equation 3.8 as follows:

$$P_{\mathrm{B}ij} - P_{\mathrm{B}i+1,j} = \frac{150\sigma^2}{(1-\sigma)^3} \cdot \frac{\mu_{\mathrm{B}ij}}{d_{\mathrm{P}}^2} Q_{\mathrm{B}ij} \quad + \frac{1.75\sigma}{(1-\sigma)^3} \cdot \frac{\rho_{\mathrm{Bi}ij}}{d_{\mathrm{P}}} Q_{\mathrm{B}ij} \cdot \frac{\Delta r}{2\pi r_i \Delta L} \tag{3.30}$$

The local feed mass balances are rewritten in a finite difference form:

$$Q_{\mathrm{B}ij} = Q_{\mathrm{B}i+1,j} + S_{ij} J_{\mathrm{V}ij} \tag{3.31}$$

$$C_{\mathrm{B}ij} Q_{\mathrm{B}ij} = C_{\mathrm{B}i+1,j} Q_{\mathrm{B}i+1,j} + S_{ij} C_{\mathrm{P}ij} J_{\mathrm{Vij}} \tag{3.32}$$

The local area inside the fiber is given by:

$$S_{ij} = 4\pi\sigma L \left(r_i^2 - r_{i-1}^2\right) / d_{\mathrm{O}} n \tag{3.33}$$

where

$$\sigma = \frac{d_{\mathrm{O}}^2 N \{\sqrt{L^2 + (\pi W D_{\mathrm{o}})^2} + \sqrt{L^2 + (\pi W D_{\mathrm{l}})^2}\}}{2L\left(D_{\mathrm{O}}^2 - D_1^2\right)} \tag{3.34}$$

The total of permeate quantity (so-called membrane productivity) is given by:

$$Q_{\mathrm{PT}} = \sum_{i=1}^{m} \sum_{j=1}^{n} \left(J_{\mathrm{V}ij} S_{ij}\right) \tag{3.35}$$

While the overall permeate concentration from which the membrane rejection is evaluated is given by:

$$C_{\mathrm{PT}} = \left\{ \sum_{i=1}^{m} \sum_{j=1}^{n} \left(C_{\mathrm{P}ij} J_{\mathrm{Vij}} S_{ij}\right) \right\} / Q_{\mathrm{PT}} \tag{3.36}$$

Membrane productivity in terms of percentage recovery can be defined as:

$$R_{\mathrm{c}} = \frac{Q_{\mathrm{PT}}}{Q_{\mathrm{f}}} \cdot 100 \tag{3.37}$$

Percentage salts rejection is given by:

$$R_{\mathrm{j}} = \left(1 - \frac{C_{\mathrm{PT}}}{C_{\mathrm{f}}}\right) \cdot 100 \tag{3.38}$$

The computer logic for the numerical solution of the FCP model is explained step-by-step in the following section. The solution follows an iterative approach that can be solved using computer software programs such as Python or MATLAB. However, Python is used in this study because it is a free, reliable and robust programming language.

Solution procedure for the FCP model in Python

The FCP model is solved by an iterative solution approach as summaries in the following steps and shown in Figure 3.8 [32].

1. Data for feed water properties, membrane dimensions, and operating conditions are input into the software.
2. Feed water flowrate (Q_f) is assumed.
3. Local membrane surface area (S_{ij}) is calculated from (Eq. 3.33).
4. The inlet permeate pressure to the fiber ($P_{\mathrm{P}in}$) is assumed.
5. Local concentration polarization coefficient (Φ_{ij}) is assumed.
6. Based on the above initial guesses, the following are calculated:
   - Local solution flux through membrane ($J_{\mathrm{v}ij}$) from (Eq. 3.23).
   - Local permeate concentration ($C_{\mathrm{P}ij}$) from (Eq. 3.26).
   - Local mass transfer coefficient (k_{ij}) from (Eq. 3.25).
   - Local concentration polarization coefficient (Φ_{ij}) from (Eq. 3.24).
7. Calculated and assumed Φ_{ij} are compared. If they are equal, the calculation is carried on to the next step, otherwise, Φ_{ij} is re-assumed and the calculation is repeated starting from step 5 until the two values be approximately equal.
8. When assumed and calculated Φ_{ij} are equal, the following are calculated:

- Local flowrate and concentration for the bulk in the feed side ($Q_{\mathrm{B}ij}$ and $C_{\mathrm{B}ij}$) from from (Eq. 3.31) and (3.32), respectively.
- Local permeate pressure inside the fiber segment ($P_{\mathrm{P}ij}$) from (Eq. 3.28).
- Local pressure in the tube sheet (P_{Pi1}) from (Eq. 3.29).

9. If P_{Pi1} equals fiber exit permeate pressure (P_{Po}), move to the next step, otherwise, re-assume $P_{\mathrm{P}in}$ and repeat the previous steps starting from step 4 until the two values be approximately equal.

10. When P_{Pi1} and P_{Po} are equal, the following are calculated:
    - Local bulk pressure on feed side ($P_{\mathrm{B}ij}$) from (Eq. 3.30).
    - Total permeate flowrate and concentration (Q_{PT} and C_{PT}) from (Eq. 3.35 and Eq. 3.36), respectively.

11. Module recovery (R_{c}) is calculated from (Eq. 3.37).

12. Calculated and assumed R_{c} are compared, if they are approximately equal, end the calculation, otherwise, assume a new Q_f and repeat the previous steps starting from step 2.

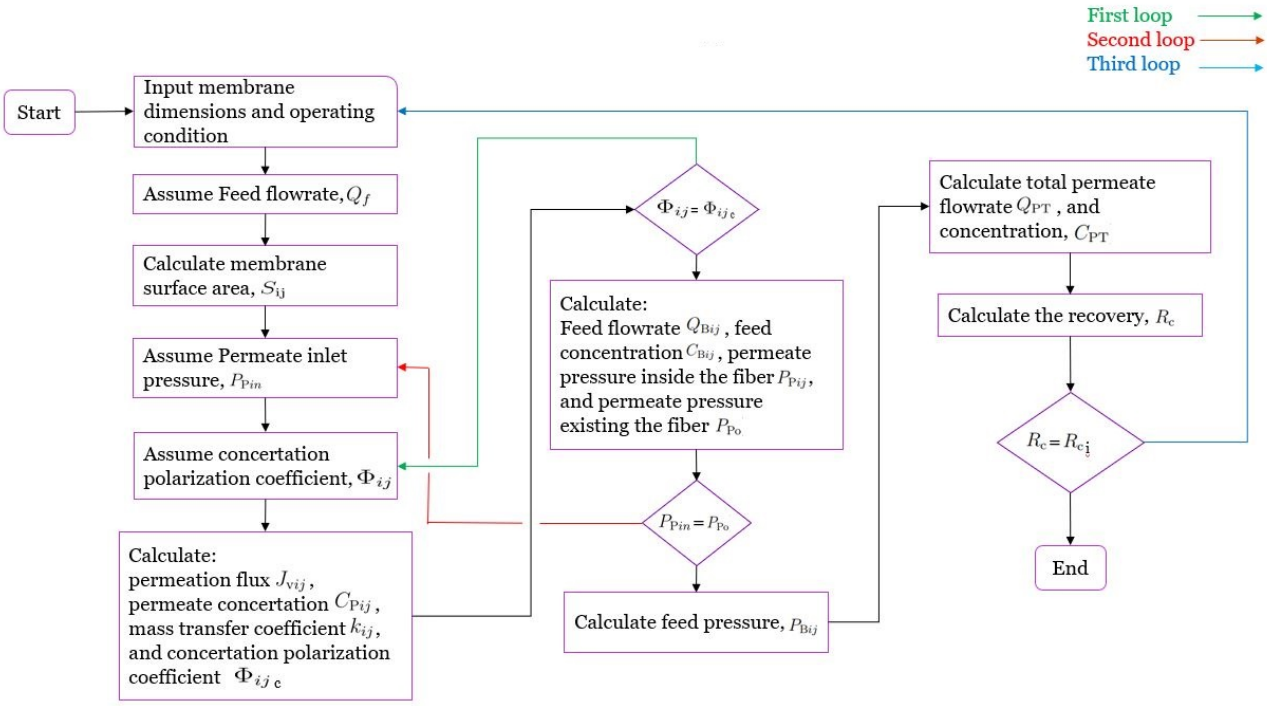

Figure 3.8: Solution algorithm for FCP model in Python

Chapter 4

Parametric studies on hollow fiber reverse osmosis membranes

The objective of this chapter is to demonstrate how various process designs and parameters may impact the quantity and quality of produced water and the brine waste from the hollow fiber seawater reverse osmosis process. Also, to quantify the brine volume associated with each process layout. As a result of this chapter, a better understating of the process at hand should be attained as well as the quantity and concentration of brine from any hollow fiber seawater reverse osmosis membranes should be easily obtained. It is the first step for reverse osmosis brine treatment process.

The following parametric studies were carried out under representative conditions as shown in Table 4.1, unless otherwise mentioned. This means, in each study, one or two parameters were changed while the rest of the parameters are fixed unless indicated specifically in the study.

Table 4.1: Simulation parameters for hollow fiber seawater reverse osmosis membranes

Simulation Parameters	
Target product water volume	5000 m^3/day
Target product salt concentration	500 ppm
Feed sea water salt concentration	35000 ppm
Membrane configuration	Hollow fiber
Membrane	Asymmetric cellulose triacetate

A single-stage hollow fiber reverse osmosis is shown in Figure 4.1, is used to demonstrate the simplest scenario for the operation of hollow fiber seawater reverse osmosis membranes to be compared later with more complicated scenarios to test the process reliability.

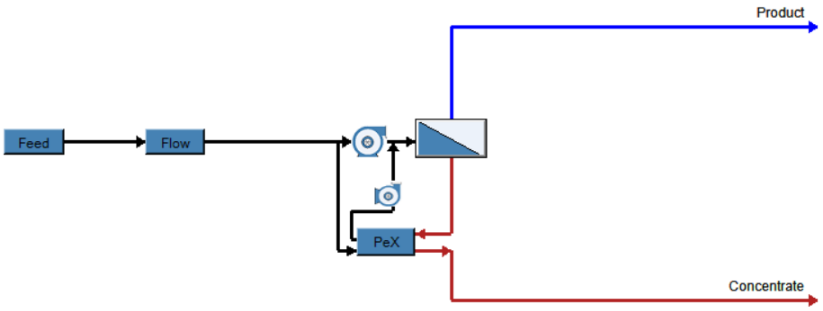

Figure 4.1: Single stage RO.

4.1 Impact of membrane permeability

Water flux through the membrane depends on the permeability coefficient of the membrane which can be determined experimentally for each membrane based on its materials [6, 32]. This study compares four hollow fibers membranes and each has a different permeability coefficient as listed in Table 4.2.

Figure 4.2 shows the adverse impact of increasing the water recovery on the water flux which increases the impact of concentration polarization. In other words, increasing recovery means increasing the feed flowrate. Since the selectivity of the membrane is kept constant, more hydraulic pressure is required to facilitate water permeation across the membrane to achieve higher recoveries. Therefore, as a result of operating at high pressures, the impact of concentration polarization may lead to membrane fouling, which reduces the membrane permeability by creating dead areas in the membrane.

Table 4.2: Permeability study conditions

Feed concentration	35000	ppm
Feed pressure	80	bar
Feed Temperature	25	°C
Membrane area	1	m^2
Permeability coefficients, $kg/m^2 \cdot s$		
Membrane 1	9.80×10^{-10}	
Membrane 2	1.08×10^{-09}	
Membrane 3	1.24×10^{-09}	
Membrane 4	1.33×10^{-09}	

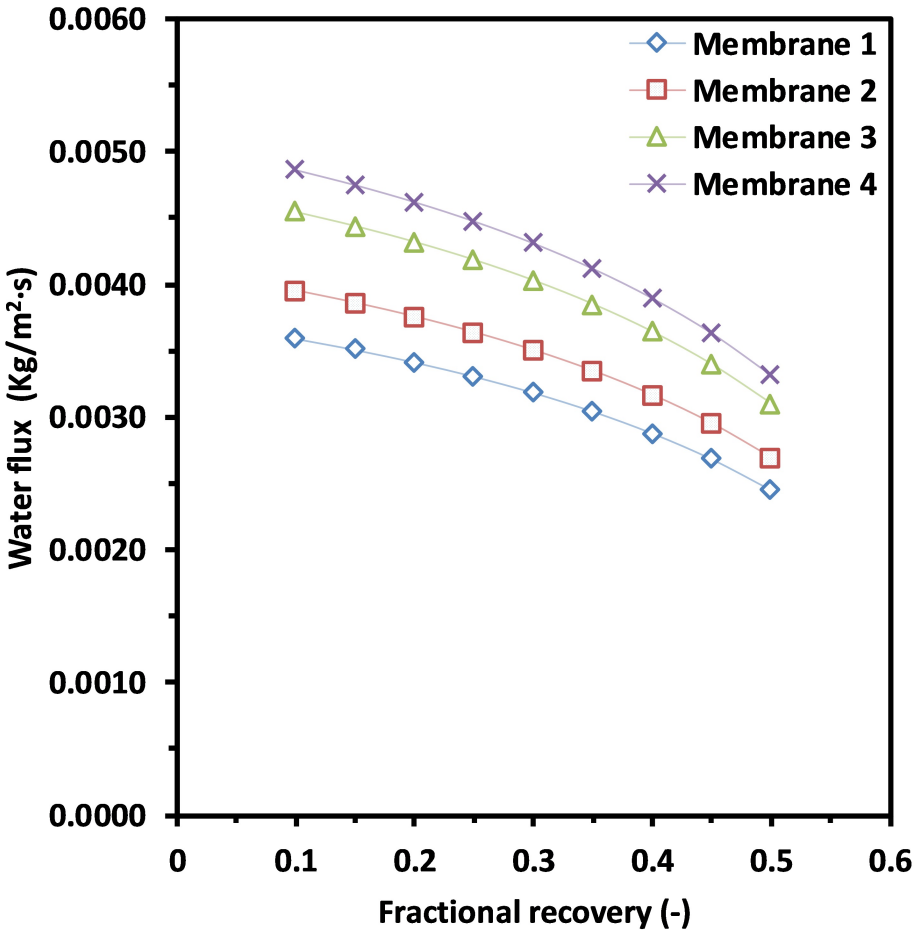

Figure 4.2: Impact of permeability on Water flux.

Theoretically, the permeability coefficient consists of diffusion and sorption coefficient which are related by equation 4.1. [6]

$$P = D \cdot K \tag{4.1}$$

Diffusion coefficient (D) quantifies the impact of the membranes (polymer) materials on the diffusing solute, while the sorption coefficient (K) relates the concentration of solutes in feed solution to the solute concentration inside the membrane. However, D contributes to a larger impact on the value of the membrane permeability coefficient (P) compared to the impact of K [6].

Table 4.3 shows an example for the change in D and K as the membrane materials changes [6]

Table 4.3: The change in D and K as the membrane material changes.

		Membrane	
Water		Cellulose diacetate	Cellulose triacetate.
Diffusion coefficient, D_w $\times 10^{-10}$	m^2/s	5.7	1.3
Sorption coefficient, K_w	-	0.29	0.12
Salt			
Diffusion coefficient, D_s $\times 10^{-12}$	m^2/s	2.90	0.00039
Sorption coefficient, K_s	-	0.17	0.015

4.2 Impact of feed concentration on the membrane rejection

In desalination applications, the quality of produced water by reverse osmosis membranes depends on membrane rejection (R), which is defined by:

$$R_{\mathrm{j}} = \left(1 - \frac{c_p}{c_f}\right) \cdot 100 \tag{4.2}$$

where c_p and c_f are the concentrations of the salt in the permeate and feed, respectively.

The salt rejection is the separation capability of the membranes to pass water and to reject salts.

Separation mechanism in reverse osmosis membranes

In Reverse Osmosis membranes, both water and salts pass across the membrane, but the rate of diffusion for water is millions of times higher than the diffusion of salts [2, 6]. Therefore, there is an accumulation of salts on the membrane surface. This leads to concentration polarization which affects water flux negatively over time.

Figure 4.3 illustrates the performance of hollow fiber seawater reverse osmosis membranes when the salt concentration in feed stream increases under conditions specified in Table 4.2. Figure 4.3 shows that salt rejection is adversely impacted by increasing salt concentration in the feed stream. This happens due to the possibility of accumulating more salts near to the surface of the membrane as the feed concentration increases which reduces the transport of water across the membrane. In addition, at a higher salt concentration in the feed water, the osmotic pressure is higher, and thus the driving force for water permeation is decreased. The opposite is true for salt permeation resulting in lower salt rejection.

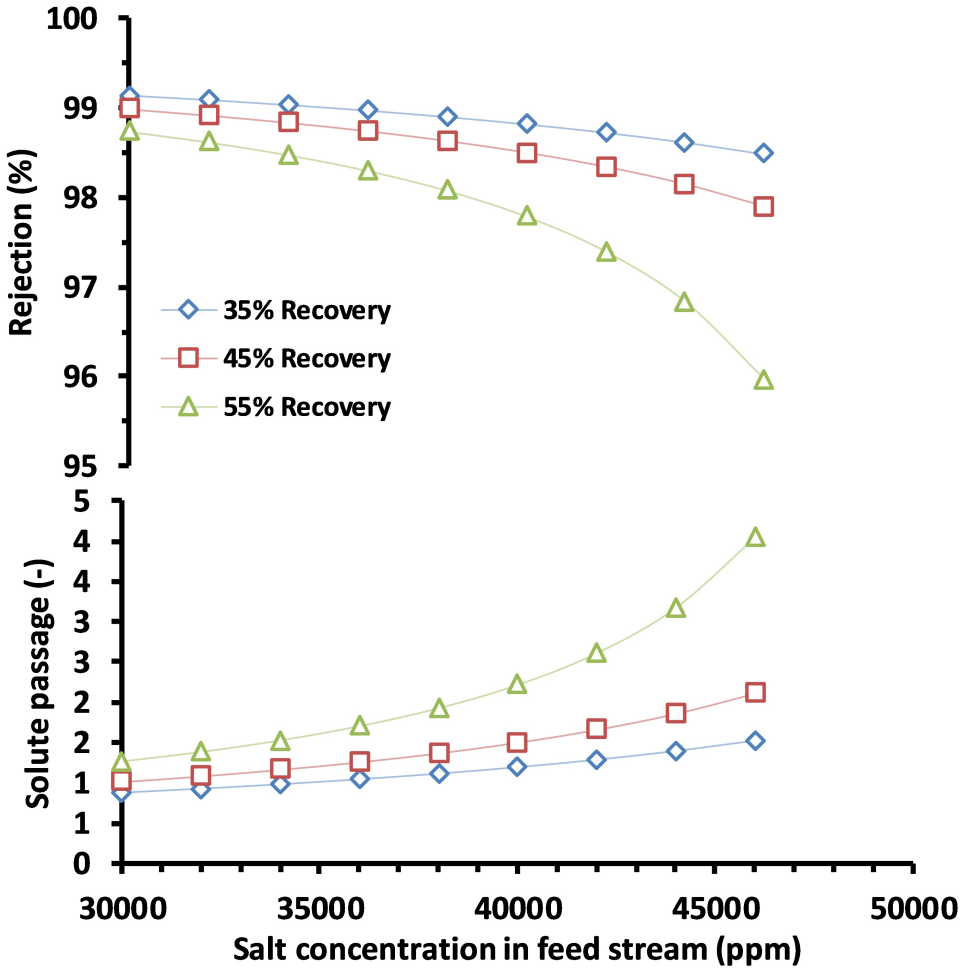

Figure 4.3: The impact of feed concentration on the membrane rejection.

Note:
The solute passage (SP) indicates how much solutes has passed through the membrane, it is defined as:

$$SP = 1 - R_{\mathrm{j}} \tag{4.3}$$

Impact of feed pressure

Feed pressure (P_f) has a strong impact on water productivity, as shown in Figure 4.4. This is consistent with the solution diffusion model [32], where feed pressure is related to water flux by the equation 3.1.

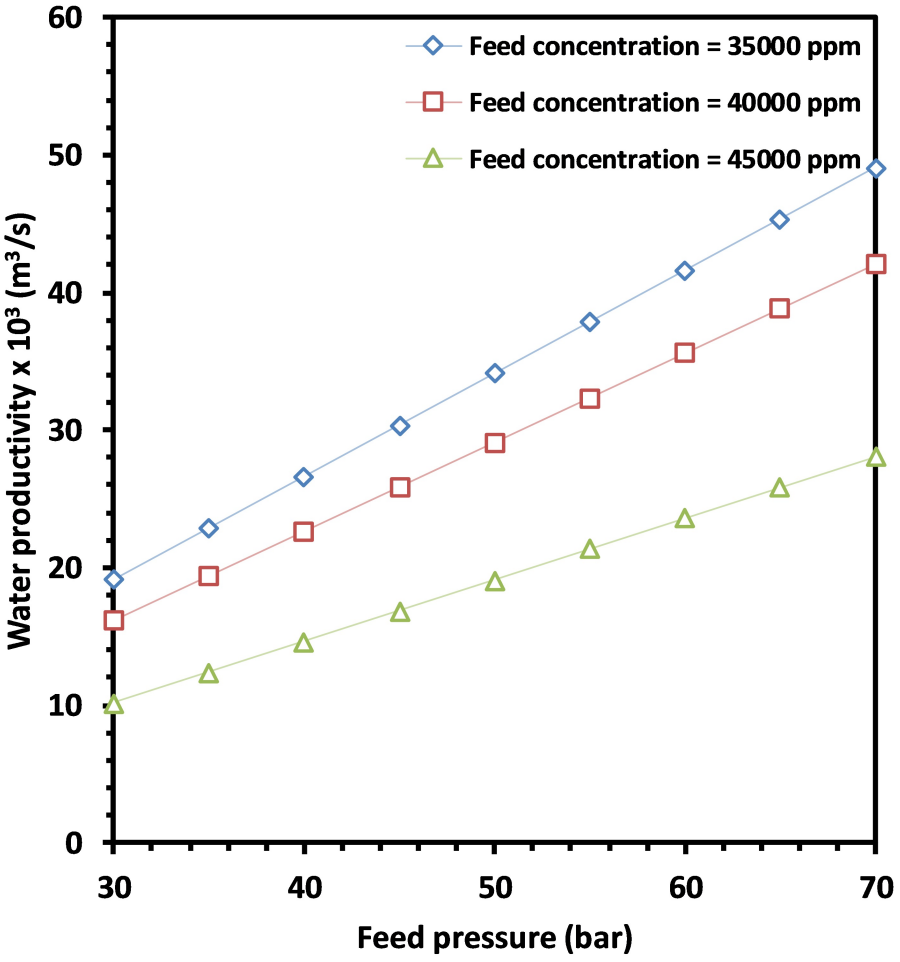

Figure 4.4: Impact of feed pressure on water productivity for feed water with different salt concentrations.

4.3 Impact of reverse osmosis Stages layout and area

The change in hollow fiber seawater reverse osmosis membranes process layout (arrangement) could lead to a considerable enhancement in the desalination performance. In industry, multiple hollow fiber seawater reverse osmosis membrane modules are used, and these modules are held together in a skid called a train. A single-stage hollow fiber seawater reverse osmosis membrane may consist of more than one train. Thus, hollow fiber seawater reverse osmosis membranes usually are split into multiple stages called passes.

The reason for multiple passes is either to recover more water or to protect the membrane. Usually, hollow fiber seawater reverse osmosis membrane manufacturers use constant area per module for each module type for easier manufacturing and standardization. Therefore, based on the water production target and the productivity of each module, the required area for certain applications is calculated.

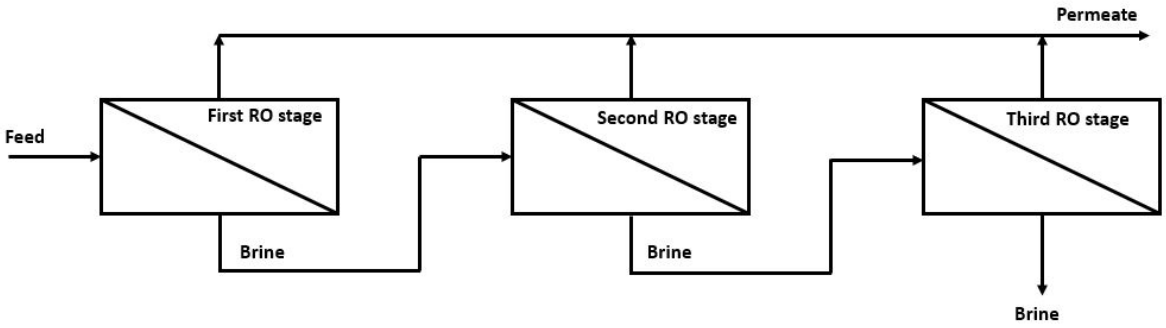

Figure 4.5: Impact of stages layout.

Arrangement for the RO stage is shown in Figure 4.5 may enhance the overall water recovery and reduce the volume of brine produced. This is related to the membrane area as shown in Figure 4.6. That is as the feed salt concentration increases, the required membrane area increases, too. In this layout, the brine from the first stage is used as a feed to the second stage, and brine from the second stage is fed to the third stage. Therefore, the membrane area required in the second stage is more than the area required in the first stage and the same for the third stage due to the increase in feed salt concentration in the second and third stages, respectively. Hence the membrane area per module is set constant by the manufacturers, more membrane modules are required to increase the area per stage based on the feed concentration and the product target. This translates to the use of more

membrane modules in the second stage than the first stage and more membrane modules in the third stage than the second stage.

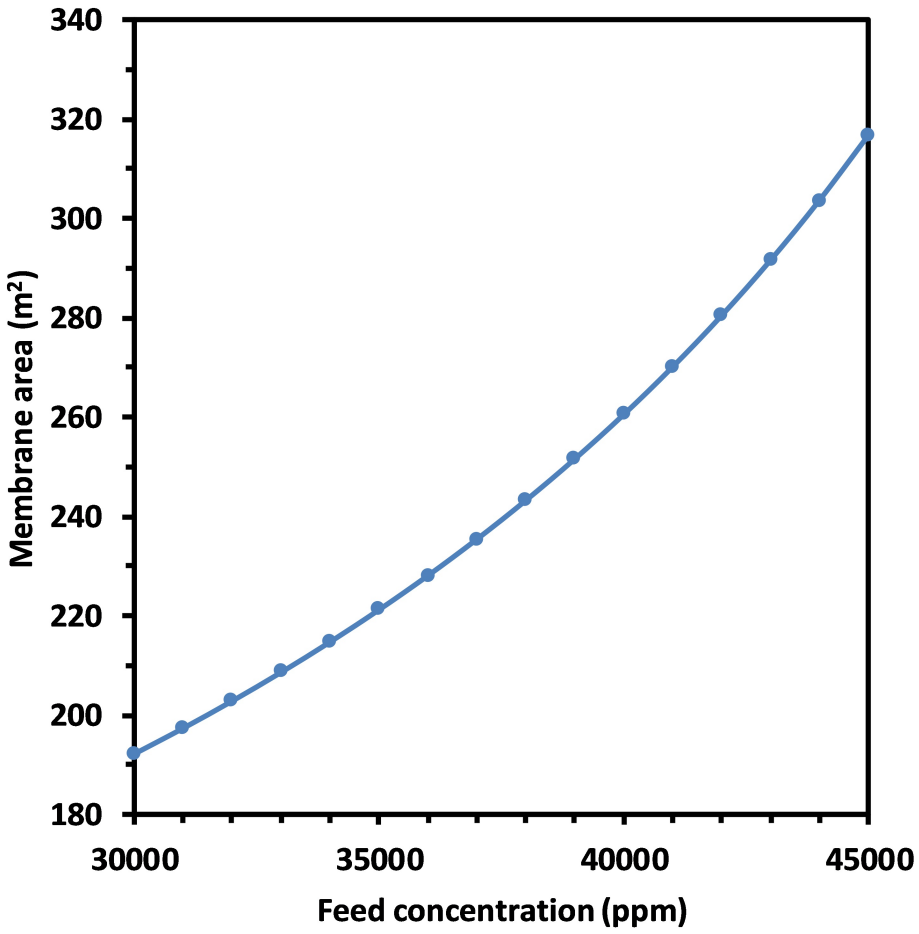

Figure 4.6: Membrane area required for different of feed salt concentrations.

Chapter 5

Brine utilization case studies

This chapter summaries the results of case studies for treating seawater reverse osmosis brine by pervaporation and membrane distillation processes. Based on the literature review, case studies are carried out to study two brine treatment options, including:

1. Reverse osmosis followed by pervaporation, RO-PV process.
2. Reverse osmosis followed by membrane distillation, RO-MD process.

The data and models used in these case studies are taken from the literature. Since PV and MD membranes are not commercialized yet, there are no precise analytical models to describe these processes. Thus, the models used here are based on actual PV and MD performance data for the type of membranes and experimental conditions. However, the objective is not to accurately find how efficient these processes are, rather forming a framework for hybrid processes capable of treating brine from seawater reverse osmosis processes. Finally, as the research develops in PV and MD, the accuracy for this framework processes is expected to enhance.

5.1 Case study: RO-PV

RO-PV study objectives and assumptions

This case study aims to find out the percentage of water produced from seawater reverse osmosis brine treated by the PV process and the percentage of salts remained after the PV.

The assumptions used [9, 20, 32]:

1. Solution diffusion model is applied to both RO and PV since they are dense membranes.
2. The pressure drop in the PV process is negligible.
3. RO process is isothermal while PV is not.
4. NaCl is the major salt concentrated in seawater reverse osmosis brine.
5. Pressure exchanger (PX) has a design efficiency of 90%.
6. The impact of fouling on RO and PV is limited due to the use of proper antifoulants.

RO-PV process description and conditions

A simple process flow diagram for the RO-PV process is shown in Figure 5.1, where the feed saline water is pressurized and fed to the RO process. Then, the permeate is taken as product water while the brine is contacted with the feed water in a pressure exchanger to recover most of its pressure. Next, a low-grade heat source such as solar heat or low-temperature steam is used to preheat the brine to the desired temperature prior to entering the PV unit.

After heating, water evaporates from brine and permeates through the PV membrane due to vapor pressure difference across the PV membrane. Meanwhile, the permeate side of the PV process is kept under a continuous vacuum to provide a driving force for permeation and to evaporate water at low temperatures on the permeate side. Thus, the produced water is taken as a product after being condensed via external condensers. Finally, the residual brine is taken out from PV as a waste that could be fed to another PV unit or to a crystallizer in order to totally separate salts from water which is not in the scope of this study.

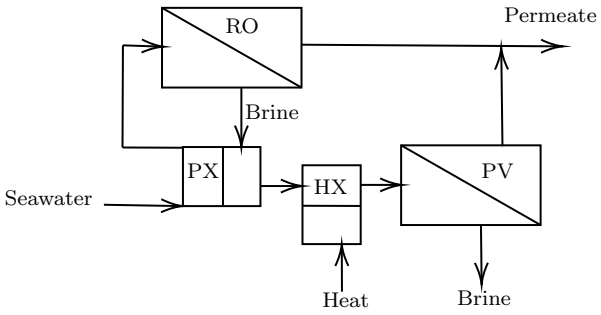

Figure 5.1: Hybrid reverse osmosis and pervaporation process (RO-PV).

Membrane and operating conditions for this case study are summarized in Table 5.1. The hollow fiber seawater reverse osmosis membrane specification data is provided by the membrane manufacturer (Toyobo Co., Ltd.) [40]. And the PV membranes data is taken from University of Waterloo thesis written by Aoran Gao. (2016) based on experimental studies in our Membrane Research Laboratory [9].

Table 5.1: RO-PV process conditions.

	Operating conditions					
	Single stage RO			Single stage PV		
	Feed	Permeate	Brine	Feed	Permeate	Brine
Concentration (ppm)	35000	140	49,940	49,940	4.99	62,424
Flowrate (m^3/day)	16,667	5,000	11,667	11,667	2333.4	9,334
Temperature (°C)	25	25	25	65	45	45
Feed pressure (bars)	53.90	2.16	51.74	5.17	5.17	5.17
	Design criteria					
Membrane type	Toyobo Hollosep HM9255			Pebax		
Membrane area per module (m^2)	0.899			0.300		
Water production per module ($m^3/m^2 \cdot day$)	35			16		
Total membrane area (m^2)	142.85			583.35		
Membrane material	Cellulose triacetate			PEBA		
Pressure drop per 1 module (%)	17			1		
Design configuration	Hollow fiber			Flat sheet		
Number of RO stages	1			1		
Salt Rejection, %	99.6			99.99		
Recovery, %	30			20		

Results and discussion

As shown in Figure 5.2, the feed inlet concentration has a negative impact on water flux through the PV membranes. However, permeate water concentration is almost constant. Therfore, salt rejection is not changed which is 99.99%.

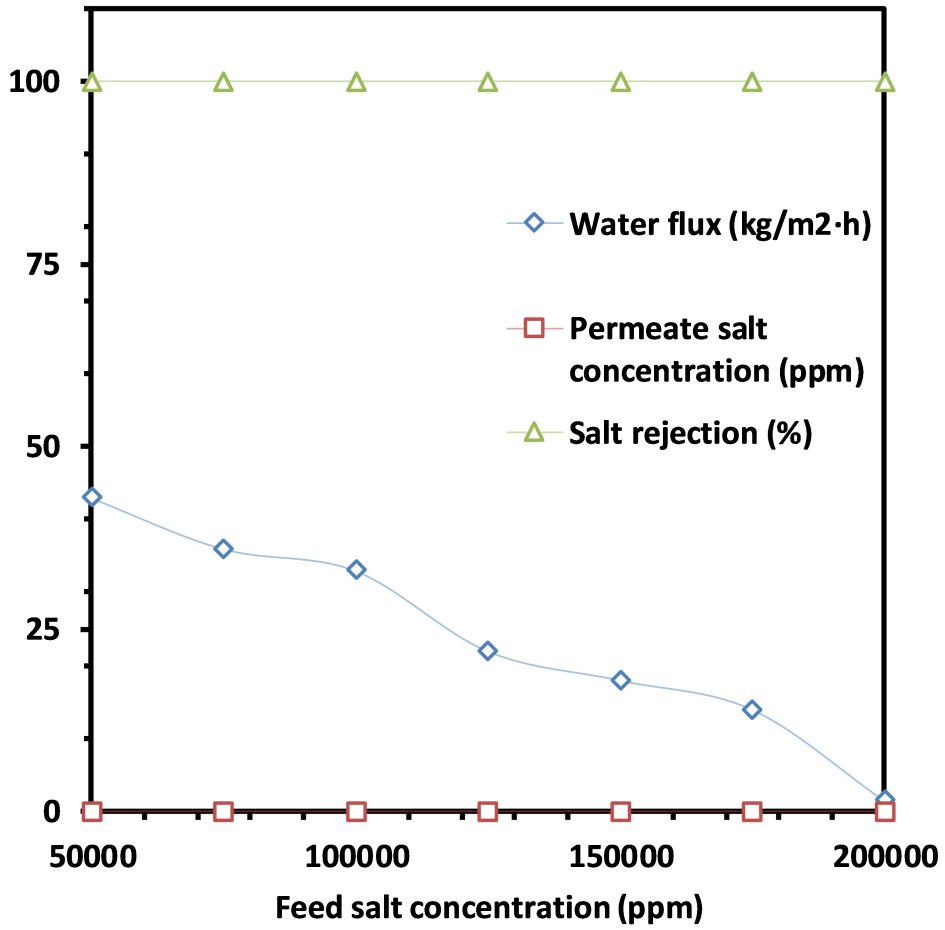

Figure 5.2: Dependence of water flux, permeate salt concentration and salt rejection on feed concentration at 65 °C in PV.

Based on the results from this case study, it can be concluded that, a single PV is capable of concentrating seawater reverse osmosis membranes brine up to 20% of its inlet salts concentration for the given conditions. This is true for feed NaCl salinity up to

200,000 ppm. Thus more than 200,000 ppm the productivity per PV stage is changed [9]. Finally, water recovered by PV is very pure due the phase change that takes place in the PV process where the non-volatile salts can hardly enter the permeate stream.

5.2 Case study: RO-MD

RO-MD study objectives and assumptions

MD can be applied for the treatment of supersaturated salty solutions including those with concentrations above their saturation point and it is feasible to be coupled with reverse osmosis desalination process [2, 23, 41, 42]. MD may contribute to achieve zero liquid discharge desalination processes [23, 43].

The objective of this study is to simulate the ability of MD to treat seawater reverse osmosis brine. Therefore, brine volume and salt concentration after reverse osmosis process is calculated first. Then, then the volume and concentration for brine after MD process is calculated.

The assumptions used [2, 15, 21]:

1. Vacuum membrane distillation is used in this study.
2. Solution diffusion model is applied for RO while pore flow model is applied for MD since MD is porous membrane.
3. The pressure drop in MD process is negligible.
4. RO process is isothermal while MD is not.
5. NaCl is the major type salt concentrated in seawater reverse osmosis brine.
6. Pressure exchanger (PX) has a design efficiency of 90%.
7. The impact of fouling on RO and MD is limited due to the use of proper antifoulants.

RO-MD process description and conditions

A simple flow diagram for RO-MD is shown in Figure 5.3. The same process order as in RO-PV is used for RO-MD for easy comparison. Brine from reverse osmosis is heated

by a low grade heat source before feeding it to MD and the evaporation occurs at the membranes surface. MD membrane is kept under vacuum, so the produced permeate can be condensed via external condensers.

However, the fundamental difference between MD and PV is that, MD uses porous and hydrophobic membranes while PV uses nonporous hydrophilic membranes. So the mass transport mechanism in MD is not the same as PV. Therefore, pore flow model is used in MD process.

In MD, the membrane acts as a medium for the liquid-vapor interface. Therefore, the pores of the membrane are kept dry of feed liquid due to the hydrophobic nature for MD membranes. But if the feed hydrostatic pressure exceeds the liquid entry pressure, the feed liquid will penetrate the membrane causing liquid breakthrough (so called membrane wetting) which hinders the separation capability of MD membranes [15].

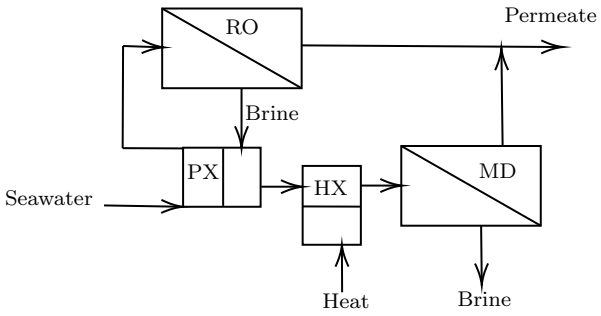

Figure 5.3: Reverse osmosis membrane distillation process flow diagram.

In this case study MD, is used to treat seawater reverse osmosis membranes brine with conditions similar to the RO-PV case study, as shown in Table 5.2. However, polytetrafluoroethylene (PTFE) membrane is used in this study.

Table 5.2: RO-MD process case study summary.

	Operating conditions					
	Single stage RO			Single stage MD		
	Feed	Permeate	Brine	Feed	Permeate	Brine
Concentration (ppm)	35000	140	49,940	49,940	4.99	62,424
Flowrate (m^3/day)	16,667	5,000	11,667	11,667	2333.4	9,334
Temperature (°C)	25	25	25	65	45	45
Feed pressure (bars)	53.90	2.16	51.74	5.17	5.17	5.17
	Design criteria					
Membrane type	Toyobo Hollosep HM9255			Pall Corp.		
Membrane area per module (m^2)	0.899			0.3		
Water production per module ($m^3/m^2 \cdot day$)	35			16		
Total membrane area (m^2)	142.85			583.35		
Membrane material	Cellulose triacetate			PTFE		
Pressure drop per 1 module (%)	0.96			0		
Design configuration	Hollow fiber			Flat sheet		
Number of RO stages	1			1		
Salt Rejection, %	99.6			99.99		
Recovery, %	30			25		

RO-MD results and discussion

At a given temperature, water flux is negatively impacted by feed salt concentration as illustrated in Figure 5.4, while the permeate concentration and the salt rejection are largely constant.

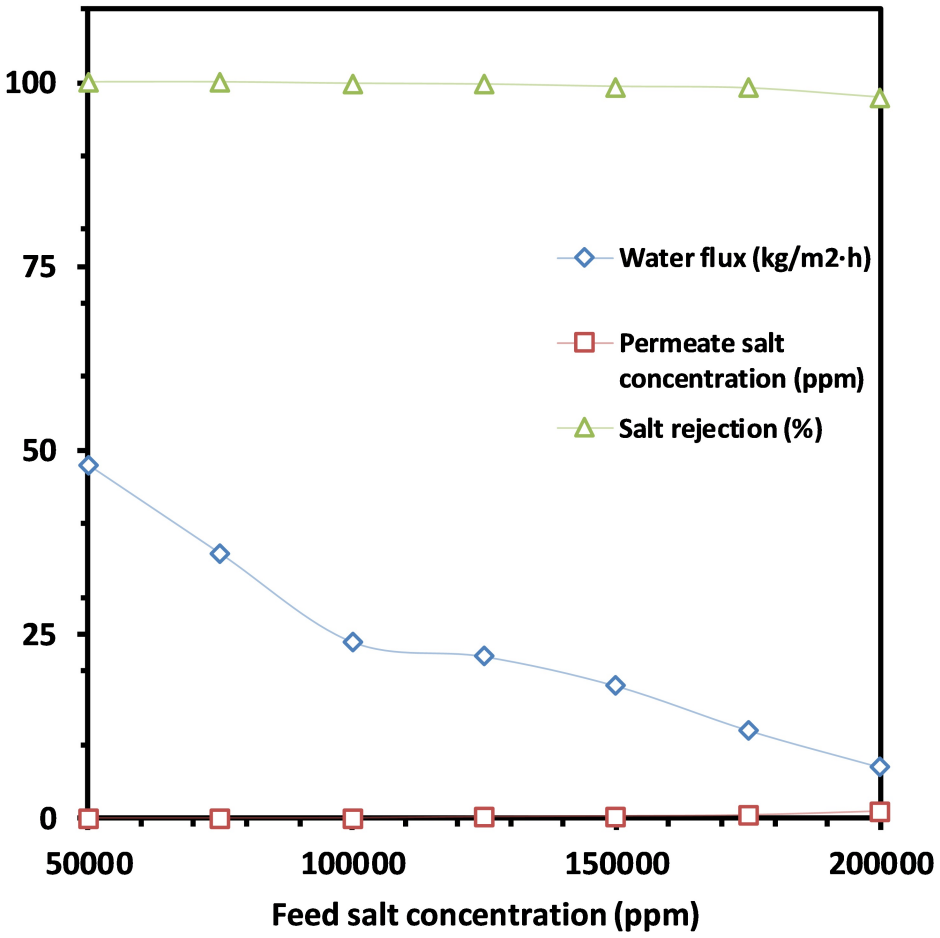

Figure 5.4: Dependence of water flux, permeate salt concentration and salt rejection on feed concentration at 65 °C in MD.

The data from this case study shows that a single MD is capable of concentrating seawater reverse osmosis membrane brine up to 25% of its inlet salts concentration for the given conditions. This is true for feed NaCl salinity up to 200,000 ppm. Thus more than

200,000 ppm the productivity per MD stage is changed [2]. Water recovered by MD is pure due to the phase change that takes place in the MD process similar to PV processes. Finally and the flux through the membrane is higher than PV due to the use of porous hydrophobic membranes.

Chapter 6

Conclusions and recommendations

6.1 General conclusions

The process of saline water desalination by reverse osmosis was studied with a focus on brine treatment. Various operating parameters impacting the operation of reverse osmosis were demonstrated. The current desalination processes discharge brine back into water bodies without treatment, and treating desalination brine is important to protect the aquatic environment and to enhance the economics of the desalination process. This research focused on treating brine with such membrane processes as pervaporation and membrane distillation.

Based on this study, PV showed higher permeate water quality than MD. On the other hand, MD showed higher water flux. Both membranes are capable of treating reverse osmosis desalination process brine up to 200,000 ppm. The major obstacles facing these emerging membrane processes are:

1. Fouling due to the increased feed salinity.
2. Withstanding high temperature because the majority of materials used are polymeric based.
3. Low water flux in pervaporation and membrane distillation as compared to reverse osmosis.
4. Concentration polarization and temperature polarization in MD which develops over time and they reduce water flux through the membrane.

6.2 Recommendations

This research acts as a skeleton for potential membrane processes that can be used to treat the brine from the reverse osmosis desalination process. However, since PV and MD are technically not fully developed, more research is needed in order to enhance the performance of these processes. This includes developing more reliable membranes at lower prices that provide high water flux and high salt rejection for industrial applications.

Besides, other processes that may be used to treat brine include crystallization and thermal evaporation. This might not be as economical as the membranes processes but they are well developed and some of them are already in use in industry. However, even these fully developed processes are not applied for desalination brine treatment on a large scale (i.e. only pilot plants available so far) primarily due to their energy-intensive disadvantage.

Another approach that may be used to limit the brine from commercial desalination processes is changing the process order. For example, a patent was filed in 2016 by SASAKURA Engineering Co., Ltd and Saline Water Conversion Corporation (SWCC) for a hybrid thermal and membrane process where the nanofiltration (NF) process is used before reverse osmosis, and then reverse osmosis brine is used as a feed for the MED desalination process. The use of the NF process allows removal of scale causing components so MED can be operated at higher temperatures to reduce the volume of brine. Hybridizing the thermal with membrane desalination processes can be another approach to reduces the brine volume from reverse osmosis desalination processes.

References

[1] El-Dessouky HT, Ettouney HM. Fundamentals of salt water desalination. Elsevier; 2002.

[2] Antonio JSR. Membrane technologies for brine treatment and membrane reuse. UNIVERSIDAD COMPLUTENSE DE MADRID; 2018.

[3] Yan Z, Yang H, Qu F, Yu H, Liang H, Li G, et al. Reverse osmosis brine treatment using direct contact membrane distillation: effects of feed temperature and velocity. Desalination. 2017;423:149–156.

[4] Edwie F, Chung TS. Development of simultaneous membrane distillation–crystallization (SMDC) technology for treatment of saturated brine. Chemical Engineering Science. 2013;98:160–172.

[5] Saudigazette. New ZLD technology turns desalination brine into valuable products; 2019. http://saudigazette.com.sa/article/571985/SAUDI-ARABIA/New-ZLD-technology-turns-desalination-brine-into-valuable-products.

[6] Baker RW. Membrane technology and applications. John Wiley & Sons; 2012.

[7] Jones E, Qadir M, van Vliet MT, Smakhtin V, Kang Sm. The state of desalination and brine production: A global outlook. Science of the Total Environment. 2018;.

[8] Panagopoulos A, Haralambous KJ, Loizidou M. Desalination brine disposal methods and treatment technologies-A review. Science of The Total Environment. 2019;.

[9] Gao A. Desalination of High-salinity Water by Membranes. University of Waterloo; 2016. Available from: https://uwspace.uwaterloo.ca/bitstream/handle/10012/10466/Gao{_}Aoran.pdf?sequence=3{&}isAllowed=y.

[10] Smith R, Purnama A, Al-Barwani H. Sensitivity of hypersaline Arabian Gulf to seawater desalination plants. Applied mathematical modelling. 2007;31(10):2347–2354.

[11] Sayyaadi H, Saffari A. Thermoeconomic optimization of multi effect distillation desalination systems. Applied Energy. 2010;87(4):1122–1133.

[12] Choi SH. On the brine re-utilization of a multi-stage flashing (MSF) desalination plant. Desalination. 2016;398:64–76.

[13] Azimi H, Thibault J, Tezel FH. Separation of Butanol Using Pervaporation: A Review of Mass Transfer Models. Journal of Fluid Flow, Heat and Mass Transfer (JFFHMT). 2019;5(4):53–82.

[14] Won W, Feng X, Lawless D. Separation of dimethyl carbonate/methanol/water mixtures by pervaporation using crosslinked chitosan membranes. Separation and purification technology. 2003;31(2):129–140.

[15] Khayet M, Matsuura T. Pervaporation and vacuum membrane distillation processes: modeling and experiments. AIChE journal. 2004;50(8):1697–1712.

[16] Korin E, Ladizhensky I, Korngold E. Hydrophilic hollow fiber membranes for water desalination by the pervaporation method. Chemical Engineering and Processing: Process Intensification. 1996;35(6):451–457.

[17] Huth E, Muthu S, Ruff L, Brant JA. Feasibility assessment of pervaporation for desalinating high-salinity brines. Journal of Water Reuse and Desalination. 2014;4(2):109–124.

[18] Liang B, Zhan W, Qi G, Lin S, Nan Q, Liu Y, et al. High performance graphene oxide/polyacrylonitrile composite pervaporation membranes for desalination applications. Journal of Materials Chemistry A. 2015;3(9):5140–5147.

[19] Bondar V, Freeman BD, Pinnau I. Gas sorption and characterization of poly (ether-b-amide) segmented block copolymers. Journal of Polymer Science Part B: Polymer Physics. 1999;37(17):2463–2475.

[20] Feng X, Huang RY. Liquid separation by membrane pervaporation: a review. Industrial & Engineering Chemistry Research. 1997;36(4):1048–1066.

[21] Alkhudhiri A, Darwish N, Hilal N. Membrane distillation: a comprehensive review. Desalination. 2012;287:2–18.

[22] Khayet M. Membranes and theoretical modeling of membrane distillation: a review. Advances in colloid and interface science. 2011;164(1-2):56–88.

[23] Martinetti CR, Childress AE, Cath TY. High recovery of concentrated RO brines using forward osmosis and membrane distillation. Journal of membrane science. 2009;331(1-2):31–39.

[24] Yip NY, Tiraferri A, Phillip WA, Schiffman JD, Elimelech M. High performance thin-film composite forward osmosis membrane. Environmental science & technology. 2010;44(10):3812–3818.

[25] Esparra-Alvarado MC. Forward Osmosis as a Reverse Osmosis Pre-treatment in Treating Brackish Water and Wastewater. Environmental Pollution Control, Pennsylvania State University. State College, PA 16801, United States; 2014.

[26] McCutcheon JR, McGinnis RL, Elimelech M. A novel ammoniacarbon dioxide forward (direct) osmosis desalination process. Desalination. 2005;174(1):1–11.

[27] Cath TY, Childress AE, Elimelech M. Forward osmosis: principles, applications, and recent developments. Journal of membrane science. 2006;281(1-2):70–87.

[28] Sarp S, Hilal N. Membrane-Based Salinity Gradient Processes for Water Treatment and Power Generation. Elsevier B.V.; 2018.

[29] Basile A, Nunes SP. Advanced Membrane Science and Technology for Sustainable Energy and Environmental Applications. Woodhead Publishing Limited; 2011.

[30] Rackley SA. Carbon Capture and Storage. 2017 Elsevier Inc.; 2017.

[31] Mendez DLM, Castel C, Lemaitre C, Favre E. Improved performances of vacuum membrane distillation for desalination applications: Materials vs process engineering potentialities. Desalination. 2019;452:208–218.

[32] Sekino M. Precise analytical model of hollow fiber reverse osmosis modules. Journal of membrane science. 1993;85(3):241–252.

[33] Lau W, Ismail A, Misdan N, Kassim M. A recent progress in thin film composite membrane: a review. Desalination. 2012;287:190–199.

[34] Matin A, Shafi H, Khan Z, Khaled M, Yang R, Gleason K, et al. Surface modification of seawater desalination reverse osmosis membranes: characterization studies & performance evaluation. Desalination. 2014;343:128–139.

[35] Ramachandhran V, Ghosh A, Prabhakar S, Tewari P. Preparation and separation performance studies on composite polyamide membranes using different amine systems and support membranes. Journal of Polymer Materials. 2009;26(2):177–185.

[36] Xu J, Yan H, Zhang Y, Pan G, Liu Y. The morphology of fully-aromatic polyamide separation layer and its relationship with separation performance of TFC membranes. Journal of Membrane Science. 2017;541:174–188.

[37] Guirguis MJ. Energy Recovery Devices in Seawater Reverse Osmosis Desalination Plants with Emphasis on Efficiency and Economical Analysis of Isobaric versus Centrifugal Devices. Department of Mechanical Engineering, University of South Florida. 4202 E Fowler Ave, Tampa, FL 33620, United States; 2011.

[38] Wan CF, Chung TS. Energy recovery by pressure retarded osmosis (PRO) in SWRO–PRO integrated processes. Applied energy. 2016;162:687–698.

[39] Sekino M. Study of an analytical model for hollow fiber reverse osmosis module systems. Desalination. 1995;100(1-3):85–97.

[40] Toyobo. HR Series and HM Series Outline Specifications;. Available from: https://www.toyobo-global.com/seihin/ro/spec-HM9255fI.htm.

[41] Tun CM, Fane AG, Matheickal JT, Sheikholeslami R. Membrane distillation crystallization of concentrated salts flux and crystal formation. Journal of Membrane Science. 2005;257(1-2):144–155.

[42] Ji X, Curcio E, Al Obaidani S, Di Profio G, Fontananova E, Drioli E. Membrane distillation-crystallization of seawater reverse osmosis brines. Separation and Purification Technology. 2010;71(1):76–82.

[43] Chen G, Lu Y, Krantz WB, Wang R, Fane AG. Optimization of operating conditions for a continuous membrane distillation crystallization process with zero salty water discharge. Journal of membrane science. 2014;450:1–11.

[44] LOEB S, SOURIRAJAN S. 9. In: Sea Water Demineralization by Means of an Osmotic Membrane;. p. 117–132. Available from: https://pubs.acs.org/doi/abs/10.1021/ba-1963-0038.ch009.

[45] Qu D, Wang J, Fan B, Luan Z, Hou D. Study on concentrating primary reverse osmosis retentate by direct contact membrane distillation. Desalination. 2009;247(1-3):540–550.

APPENDICES

Appendix A

Physical Properties and correlations

A.1 Osmotic Pressure

A.2 Water density

Density of saline water can be correlated precisely by the following correlation A.1 which is valid over salinity range of $0 \leq \mathrm{X} \leq 160000$ ppm and temperature range of $10 \leq \mathrm{T} \leq 180°\mathrm{C}$ [1]:

$$\rho = 10^3 \left(\mathrm{A_1F_1} + \mathrm{A_2F_2} + \mathrm{A_3F_3} + \mathrm{A_4F_4}\right) \tag{A.1}$$

Where
$\rho =$ saline water density in kg/m^3
X is the concentration of salts in the saline water

$B = ((2)(X)/1000 - 150)/150$
$G_1 = 0.5$
$G_2 = B$
$G_3 = 2B^2 - 1$
$A_1 = 4.032219G_1 + 0.115313G_2 + 3.26 \times 10^{-4}G_3$
$A_2 = -0.108199G_1 + 1.571 \times 10^{-3}G_2 - 9x10^{-6}G_3$
$A_4 = -0.92 \times 10^{-4}G_1 - 8.7 \times 10^{-5}G_2 - 5.3 \times 10^{-5}G_3$
$A = ((2)(T) - 200)/160$
$F_1 = 0.5$
$F_2 = A$
$F_3 = 2A^2 - 1$
$F_4 = 4A^3 - 3A$

A.3 Water dynamic viscosity

Dynamic viscosity for water can be calculated using the following A.2 correlation [1, 2]:

$$\mu = (\mu_W)(\mu_R) \times 10^{-3} \tag{A.2}$$

This correlation is valid for temperature range of $10 \leq T \leq 180$ o C and $0 \leq \mathbf{s} \leq 130$gm/kg, Where
μ = saline water's dynamic viscosity, $kg/m \times s$
s = salt concentration, g/kg
$\text{Ln}(\mu_W) = -3.79418 + 604.129/(139.18 + T)$
$\mu_R = 1 + As + Bs^2$
$A = 1.474 \times 10^{-3} + 1.5x10^{-5}T - 3.927 \times 10^{-8}T^2$
$B = 1.0734 \times 10^{-5} - 8.5 \times 10^{-8}T + 2.23 \times 10^{-10}T^2$

Glossary

antifoulants Materials used to prevent or minimize biofouling which is the accumulation of microorganisms on membrane surface such as sodium hypochlorite. 2, 5

antiscalants Called also scale inhibitors which are organic compounds used to avoid or minimize precipitation of chemicals on metal surface at high temperatures such polyphosphates, phosphonates and polycarbonic acids. 2, 5

benthic organisms Organisms that live at the bottom of the oceans, seas and lakes such as sponges, corals and sea stars. 5

brine Liquid waste concentrate of desalination processes, typically high in salts and chemicals concentrations 1

coagulants Substances that causes colloidal solid particles in a liquid solution to coagulate by neutralizing the negative electrical charge on particles such as polyamines and PolyDADMACs. 5

flocculants Chemical compounds which promotes clumping of the destabilized particles together and cause them to agglomerate and drop out of solution such as aluminum chloride, sodium aluminate and ferric chloride. 5

multi-effect distillation (MED) A distillation process often used for sea water desalination. It consists of multiple stages or "effects". In each stage the feed water is heated by steam in tubes, usually by spraying saline water onto them. 1

multi-stage flashing (MSF) A water desalination process that distills sea water by flashing a portion of the water into steam in multiple stages within an evaporator. 1

reverse Osmosis (RO) Water purification process that uses a partially permeable membrane to remove ions, unwanted molecules and larger particles from drinking water. 1

water bodies Any natural water resources such as oceans, seas, lakes, rivers and wetlands 5